AD NUMBER

ADB284977

NEW LIMITATION CHANGE

TO

Approved for public release, distribution unlimited

FROM

Distribution authorized to U.S. Gov't. agencies only; Proprietary Info.; Jun 2002. Other requests shall be referred to U.S. Army Medical Research and Materiel Command, 504 Scott St., Ft. Detrick, MD 21702-5012.

AUTHORITY

USAMRMC ltr, dtd 15 May 2003

AD_____

Award Number: DAMD17-98-1-8198

TITLE: Roles of Breast Cancer Genes in DNA Homologous Recombination and Cellular Sensitivity to Radiation and Anticancer Drugs

PRINCIPAL INVESTIGATOR: Zhiyuan Shen, M.D., Ph.D.

CONTRACTING ORGANIZATION: University of New Mexico Health Sciences Center
Albuquerque, New Mexico 87131

REPORT DATE: June 2002

TYPE OF REPORT: Final

PREPARED FOR: U.S. Army Medical Research and Materiel Command
Fort Detrick, Maryland 21702-5012

NOTICE

USING GOVERNMENT DRAWINGS, SPECIFICATIONS, OR OTHER DATA INCLUDED IN THIS DOCUMENT FOR ANY PURPOSE OTHER THAN GOVERNMENT PROCUREMENT DOES NOT IN ANY WAY OBLIGATE THE U.S. GOVERNMENT. THE FACT THAT THE GOVERNMENT FORMULATED OR SUPPLIED THE DRAWINGS, SPECIFICATIONS, OR OTHER DATA DOES NOT LICENSE THE HOLDER OR ANY OTHER PERSON OR CORPORATION; OR CONVEY ANY RIGHTS OR PERMISSION TO MANUFACTURE, USE, OR SELL ANY PATENTED INVENTION THAT MAY RELATE TO THEM.

LIMITED RIGHTS LEGEND

Award Number: DAMD17-98-1-8198
Organization: University of New Mexico Health Sciences Center

Those portions of the technical data contained in this report marked as limited rights data shall not, without the written permission of the above contractor, be (a) released or disclosed outside the government, (b) used by the Government for manufacture or, in the case of computer software documentation, for preparing the same or similar computer software, or (c) used by a party other than the Government, except that the Government may release or disclose technical data to persons outside the Government, or permit the use of technical data by such persons, if (i) such release, disclosure, or use is necessary for emergency repair or overhaul or (ii) is a release or disclosure of technical data (other than detailed manufacturing or process data) to, or use of such data by, a foreign government that is in the interest of the Government and is required for evaluational or informational purposes, provided in either case that such release, disclosure or use is made subject to a prohibition that the person to whom the data is released or disclosed may not further use, release or disclose such data, and the contractor or subcontractor or subcontractor asserting the restriction is notified of such release, disclosure or use. This legend, together with the indications of the portions of this data which are subject to such limitations, shall be included on any reproduction hereof which includes any part of the portions subject to such limitations.

THIS TECHNICAL REPORT HAS BEEN REVIEWED AND IS APPROVED FOR PUBLICATION.

_____ _____

_____ _____

REPORT DOCUMENTATION PAGE

Form Approved
OMB No. 074-0188

1. AGENCY USE ONLY (Leave blank)	2. REPORT DATE	3. REPORT TYPE AND DATES COVERED
	June 2002	Final (1 Sep 99 - 30 May 02)

4. TITLE AND SUBTITLE
Roles of Breast Cancer Genes in DNA Homologous Recombination and Cellular Sensitivity to Radiation and Anticancer Drugs

5. FUNDING NUMBERS
DAMD17-98-1-8198

6. AUTHOR(S)
Zhiyuan Shen, M.D., Ph.D.

7. PERFORMING ORGANIZATION NAME(S) AND ADDRESS(ES)
University of New Mexico Health Sciences Center
Albuquerque, New Mexico 87131

E-Mail: zshen@salud.unm.edu

8. PERFORMING ORGANIZATION REPORT NUMBER

9. SPONSORING / MONITORING AGENCY NAME(S) AND ADDRESS(ES)
U.S. Army Medical Research and Materiel Command
Fort Detrick, Maryland 21702-5012

10. SPONSORING / MONITORING AGENCY REPORT NUMBER

11. SUPPLEMENTARY NOTES
report contains color

12a. DISTRIBUTION / AVAILABILITY STATEMENT
Distribution authorized to U.S. Government agencies only (proprietary information, Jun 02). Other requests for this document shall be referred to U.S. Army Medical Research and Materiel Command, 504 Scott Street, Fort Detrick, Maryland 21702-5012.

12b. DISTRIBUTION CODE

13. Abstract *(Maximum 200 Words)* *(abstract should contain no proprietary or confidential information)*

Mutations of the BRCA2 and BRCA1 tumor suppressor genes predispose humans to many forms of cancer, including breast and ovarian cancer. It has been suggested that BRCA1 and BRCA2 may serve as "caretakers" to repair DNA by interacting with RAD51. It is also possible that BRCA1 and BRCA2 interact with additional proteins to accomplish their functional roles in tumor suppression. We have focused our study on BRCA2. The first objective is to further characterize the role of BRCA2 in DNA homologous recombination and cellular sensitivity to DNA damage. Although the interactions between exon 11 of human BRCA2 with RAD51 have been extensively reported, little is known about the interaction between RAD51 and the C-terminal domain coded by exon 27 of BRCA2. We clarified the interaction between RAD51 and this C-terminal region of human BRCA2, and further demonstrated that its overexpression inhibits DNA double strand break-induced homologous recombination. The second objective is to identify new proteins that may interact with BRCA2. We have identified two new BRCA2-interacting proteins, BCCIP and ABP-280/filamin-1. We have performed extensive characterization on these interactions and published 2 papers and submitted another.

14. SUBJECT TERMS	15. NUMBER OF PAGES
breast cancer	62
	16. PRICE CODE

17. SECURITY CLASSIFICATION OF REPORT	18. SECURITY CLASSIFICATION OF THIS PAGE	19. SECURITY CLASSIFICATION OF ABSTRACT	20. LIMITATION OF ABSTRACT
Unclassified	Unclassified	Unclassified	Unlimited

Table of Contents

A. Introduction

Mutations of the BRCA2 and BRCA1 tumor suppressor genes predispose humans to many forms of cancer, including breast and ovarian cancer. Although it has been suggested that BRCA2 and BRCA1 may serve as "caretakers" to repair DNA by interacting with RAD51, it is possible that they interact with additional proteins to accomplish their functional roles in tumor suppression. The ultimate goal of our research is to elucidate the mechanisms by which BRCA1/2 suppresses mammary tumorigenesis. This IDEA project has two scientific objectives.

- The first objective is to further characterize the functional role of breast cancer genes in recombinational DNA repair and cellular sensitivity to therapeutic DNA damage agents. We have encountered some difficulties to establish stable cell lines overexpressing dominant negative BRCA fragments. The technical approach was modified accordingly and our original scientific goals have been achieved. Unpublished data will be presented in this report.
- The second objective is to isolate and characterize additional BRCA-interacting protein(s). We have identified and characterized two new BRCA2-interacting proteins. The results of this study have been summarized in two peer-reviewed publications, and another submitted manuscript. We will briefly describe this study. The details can be found in appendices.

B. Body of final report

B1. Objective 1 (tasks 1, 2, 3 and 4), functional roles of BRCA in recombination repair.

The objective of tasks 1-4 is to investigate whether overexpression of dominant negative BRCA (dnBRCA) inhibits DNA homologous recombination and sensitizes cells to DNA damage. Although it is known that both BRCA1 and BRCA2 associate with RAD51 protein (1-5), it is controversial whether BRCA1 directly binds to RAD51 (for a review, see (6)). Therefore, we have directed our effort to focus on BRCA2 protein.

Interaction of the C-terminal domain of human BRCA2 with RAD51. The BRCA2 protein contains two putative regions for RAD51 interactions. One is coded by exon 11 that contains several BRC repeats. The other is coded by exon 27. We originally focused on several BRC repeats of BRCA2 protein (see Annual Report 1999). During the course of these studies, several labs reported that the overexpression of the BRC repeats coded by exon 11 of BRCA2 sensitizes cells to DNA damage and inhibits recombinational repair (3, 5, 7, 8). Therefore, we are less enthusiastic about exon 11 in order to avoid repeating the published studies. Although it was reported that the region coded by exon 27 of mouse BRCA2 interacts with RAD51 (2), it has not been confirmed whether the corresponding region of human BRCA2 also interacts with RAD51. It is not known whether this putative RAD51-interacting domain also plays a role in the regulation of recombinational DNA repair. Therefore, we focused our attention to the putative C-terminal RAD51 binding domain of human BRCA2. We made two fragments that contain this region, designated BRCA2-A (amino acids 3206-3310) and BRCA2-D (amino acids 3179-3418). BRCA2-A

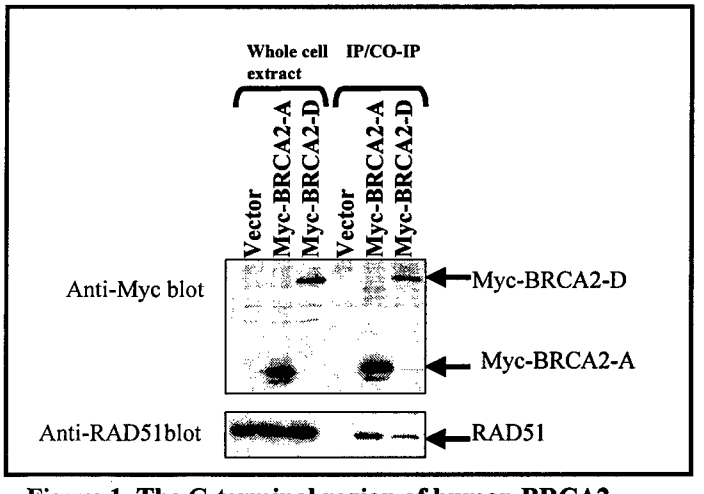

Figure 1. The C-terminal region of human BRCA2 protein interacts with RAD51. Myc-tagged BRCA2-A or BRCA2-D was expressed in HeLa cells. The whole cell extract was precipitated with anti-Myc antibodies. Precipitated Myc-tagged proteins were detected by anti-Myc blot (top panel), and co-precipitated RAD51 was detected by anti-RAD51 blot (bottom panel). See text for more details.

corresponds to the mouse RAD51-interacting region (2). The BRCA2-D contains the C-terminal 240 amino acids of human BRCA2, including the putative RAD51-interacting region. We tested whether these fragments interact with human RAD51. As shown in Figure 1, both BRCA2-A and BRCA2-D can co-precipitate endogenous RAD51 protein. These data confirmed that the C-terminal region of human BRCA2 interacts with RAD51, providing bases for further studies (see bellow).

Task 1 was to establish stable cell lines with impaired BRCA2 function. The original design was to construct stable cell lines that overexpress dnBRCA by plasmid transfection. As reported in the 1999 annual report, we constructed several dnBRCA2 constructs, and failed to produce stable cell lines that overexpress these dnBRCA2 by using the strategies outlined in the original proposal. Therefore, we redirect this project to use retroviral infection in HT1080 cells, since HT1080 cells are very permissive to retrovirus. This redirection was proposed in previous annual reports and was approved by USAMRMC. We attempted retroviral infection to construct stable cell lines that express BRCA2-A or BRCA2-D. Similar to the plasmid transfection approach, the cell lines infected with the virus expressing BRCA2-A and BRCA2-D were not stable. We attribute this to the potential inhibitory effect of these fragments on cell growth. Since it is known that RAD51 protein is required for the cells to maintain normal growth, it is possible that overexpression of the RAD51-interacting domain may have impaired RAD51 function, thus inhibiting cell growth. Although this technical difficulty restricted us from doing more comprehensive analysis, it informs us that these BRCA2 regions possess important functions in cell growth control.

Tasks 2 and 3. To measure the spontaneous and double strand break (DSB)-induced homologous recombination in cells with impaired BRCA2 function. We originally planed to use stable cell lines established in task 1 to measure spontaneous and DSB-induced recombination. As described in task 1, we attempted both plasmid transfection and retroviral infection to construct stable cell lines expressing dnBRCA2, and failed. Therefore, we redirected the research to transiently co-transfect the plasmids expressing dnBRCA2. We collaborated with Dr. Mark Brenneman (formerly at Los Alamos National Laboratory, and now at University of New Mexico) to test the recombination in HT1080-1885 cells

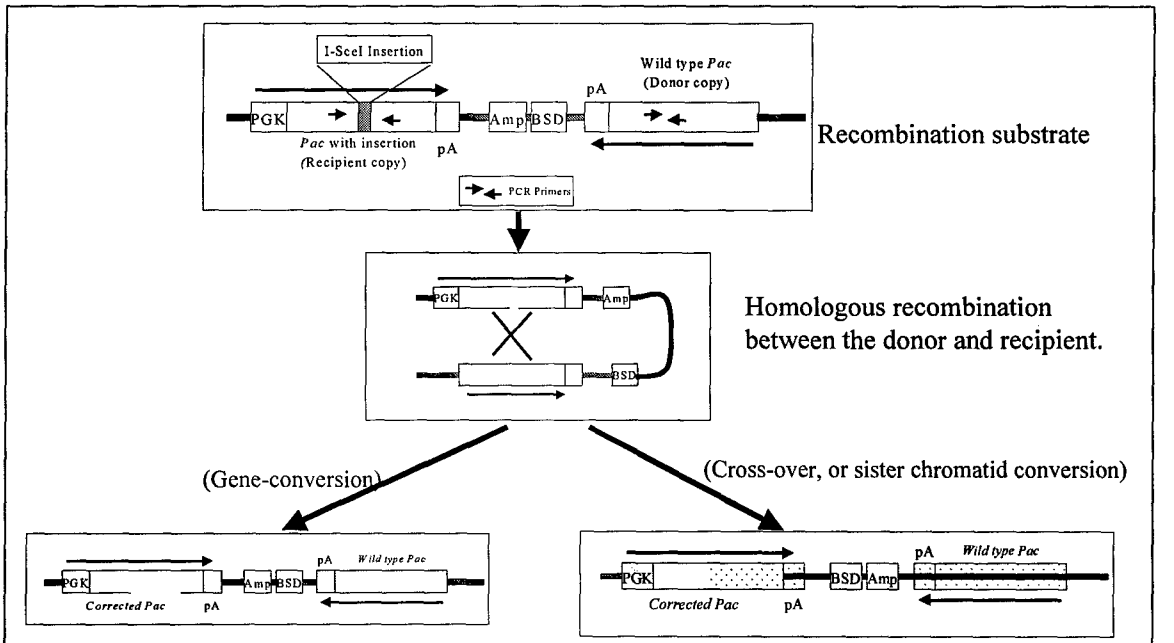

Resolving by gene conversion (left) or cross-over (right) result in restoration of a functional *pac* gene at the recipient locus.

Figure 2, the Pac recombination locus in HT1080-1885 cells.

(annual reports 1999 and 2000).

The cell system (HT1080-1885), generated by Dr. Mark Brenneman, is a human fibrosarcoma cell line that contains a recombination substrate organized as inverted repeats of the puromycin gene, *Pac* (illustrated in Figure 2). The recipient copy of *pac* expresses a truncated puromycin gene of no function due to the insertion of an I-SceI endonuclease site. The donor copy of *pac* encodes a wild type puromycin gene, but is not expressed as it lacks a promoter. When a plasmid expressing I-SceI (p3NLS-I-SceI) endonuclease is transfected, a DSB on the recipient *pac* gene can be introduced and thus a recombination between the donor and recipient copy may occur. This will result in a functional *pac* gene, conferring puromycin resistance. Therefore, the appearance of puromycin-resistant phenotype represents a HR event at the *pac* locus in the cells.

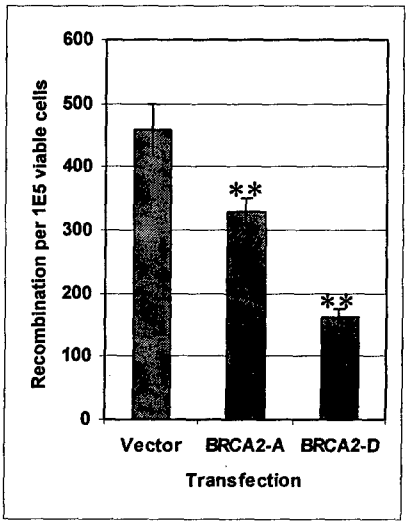

Figure 3. Overexpressions of BRCA2-A and BRCA-2D fragments inhibit DSB-induced homologous recombination. See text for details.

In collaboration with Dr. Brenneman, we co-transfected BRCA2-A and BRCA2-D with p3NLS-I-SceI into the cells, and measured the recombination frequency. As shown in Figure 3, expressions of BRCA2-A and BRCA2-D significantly inhibit DSB-induced homologous recombination. Therefore, this data suggest that the C-terminal RAD51-interacting domain is involved in the regulation of recombination. Since no stable cell lines can be constructed, spontaneous recombination frequency was not measured.

Task 4 is to determine whether the overexpression of dominant negative BRCA sensitizes cells to DNA damage. Since no stable cell line was obtained, it was technically difficult to measure cellular sensitivity to the DNA damage agent by using colony formation assay. Therefore, this task was not attempted. However, the inability to construct stable cell line expressing dnBRCA2 itself suggests that the cells are sensitive to the dnBRCA2. It implies that the BRCA2 function is essential for cell growth.

In conclusion, our study focuses on the C-terminal RAD51 interacting region of BRCA2. We have shown that this domain of human BRCA2 protein interacts with RAD51. By using a transient transfection approach, we found that the C-terminal RAD51-interacting domain regulates DSB-induced homologous recombination. To date, these results are the first to report that the human C-terminal domain of human BRCA2 associate with RDA51 and regulate recombinational repair. Although the attempt to construct stable cell lines overexpressing this domain has failed, it suggests an important role of this region for cell growth control.

B2. Objective 2 (task 5), identification of new BRCA-interacting proteins.

The objective was to identify new proteins that may interact with BRCA2 or BRCA1. As justified in section B1 (page 4), we have concentrated our effort on BRCA2. We used a conserved region of BRCA2 as the bait in a yeast two-hybrid system, and identified two important proteins that interact with BRCA2, BCCIP and filamin-1. The details of these studies are published (appendices 1-3). Briefly, BCCIP is a BRCA2, CDKN1A (Cip1/p21) - Interacting Protein, that has no significant homology to any known proteins. We have found that BCCIP gene is located at chromosome 10q26.1, a region associated with many human tumors, including advanced brain tumors, endometrial tumors, advanced prostate cancer, and some breast cancer. We also found that expression of BCCIP inhibits cell growth due to a delayed G1-S transition (Appendices 1 and 3), suggesting an important role for BCCIP in the regulation of cell growth

and proliferation. The second BRCA2-interacting protein is the previously known protein, ABP-280 or filamin-1, which is an actin binding protein. We have found, for the first time, that this protein is also involved in DNA damage response. For more details, please see appendix 2. This study suggests an interplay of the DNA repair pathway with the cytoskeleton system.

B3. Objective 3, publications and grant application (task 6).

The objective of task 6 is to summarize data, and write new grant application based on the IDEA project. We have published two papers and submitted another (see appendix 1-3). In collaboration with Dr. Brenneman, we anticipate that another manuscript describing the data of C-terminal RAD51 binding domain of BRCA2 will be submitted. Based on the results of this IDEA project, the PI has secured a DOD-BRCP CDA award entitled "BRCA2-interacting proteins and breast cancer intervention." (06/01/2002-05/30-2006, annual direct cost: ~59K). In addition, we have submitted a new NIH R01 grant application (see section D6 for details).

B4. Personnel receiving pay from their research effort

- Zhiyuan Shen, PI
- Wenhui Li, postdoctoral fellow
- Jingmei Liu, research scientist
- Xiangbing Meng, postdoctoral fellow

C. Key Research Accomplishments

- Confirmed the interaction of the C-terminal region of the human BRCA2 with RAD51.
- Discovered that the C-terminal RAD51 interacting region regulates recombinational repair.
- Isolated a new BRCA2 interacting gene, BCCIP, which is involved in regulation of cell cycle control.
- Discovered that the actin-binding protein ABP280/filamin-1 interacts with BRCA2, and identified a role of cytoskeleton proteins in DNA damage response.

D. Reportable Outcomes

D1. Manuscripts and abstracts, presentation:

Publications (see appendix for details).

1. Liu, J., Yuan, Y., Huan, J., and Shen, Z. 2001. Inhibition of brain and breast cancer cell growth by BCCIPα, an evolutionarily conserved nuclear protein that interacts with BRCA2. **Oncogene**, 20:336-345.
2. Yuan, Y., and Shen, Z. 2001. Interaction with BRCA2 suggests a role of filamin-A (hsFLNa) in DNA damage response. **J. Biol. Chem.** 276: 48318-48324.

Submitted manuscript (see appendix for full text)

3. Meng, X., Liu, J., Xu Guo, and Shen, Z. 2002. Genomic structure of the human BCCIP gene and its role in G1-S transition. Reversion submitted to **Oncogene**.

Abstracts were presented at national conferences.

4. Shen, Z., Yuan, Y., Liu, J., Hesabi, B., and Huan, J. 2000. Identification of a novel BRCA2 associated protein. Era of Hope, Department of Defense Breast Cancer Research Program Meeting. Atlanta, Georgia.
5. Liu, J., Yuan, Y., and Shen, Z. 2001. A novel BRCA2-interacting protein inhibits tumor cell growth. Forty-eighth Annual Meeting of the Radiation Research Society. San Juan, Puerto Rico.
6. Yuan, Y., and Shen, Z. 2001. Roles of actin-binding protein ABP-280 in cellular sensitivity to

irradiation. Gordon Research Conference – Radiation Oncology, Ventura, CA.

7. Liu, J., Guo, X., and Shen, Z. 2001. BCCIPα, a candidate tumor suppressor interacting with BRCA2. Gordon Research Conference – Radiation Oncology, Ventura, CA.
8. Brenneman MA, Guo, X, Wagener BM, Miller CA, Shen Z., Chen DJ, and Nickoloff JA. 2002. Interactions between BRCA2 and RAD51 govern homologous recombinational repair in human cells. Symposium on Molecular Mechanisms of DNA Replication and Recombination, Keystone Symposia, Snowbird, Utah.
9. Xiangbing Meng, Zhiyuan Shen, 2002. Interaction of BCCIP with PCNA and transcription factors. Forty-ninth Annual Meeting of the Radiation Research Society, Reno, Nevada.
10. Xu Guo, and Zhiyuan Shen, 2002. Structural and functional characterization of BCCIP, a BRCA2-interacting protein. Forty-ninth Annual Meeting of the Radiation Research Society, Reno, Nevada.
11. Yuan Yuan and Zhiyuan Shen, 2002. A role of filamin-1 in the adaptation of G2 arrest following irradiation. Forty-ninth Annual Meeting of the Radiation Research Society, Reno, Nevada.
12. Xiangbing Meng, Xu Guo, Jingmei Liu, Zhiyuan Shen. 2002. Functional characterization of BCCIP, a BRCA2-interactingprotein. Era of Hope breast cancer research meeting. Orlando, FL.

D2. Patents and licenses applied for and/issued:

None.

D3. Degree obtained:

None.

D4. Development of cell lines, tissue or serum repositories:

None.

D5. Informatics such as databases and animal models:

None.

D6. Funding applied for based on work supported by this award.

Funded new project

Funding agency: US MRMC-BCRP
Grant number: DAMD17-02-1-0515
Fund amount: ~$59K/year
Funding period: 06/01/2002-05/30/2006
Title: BRCA2-interacting proteins and breast cancer intervention
Description: This is a Career Development Award (CDA) that supports PI salary in order to relieve the PI from other academic commitments to focus on developing more breast cancer research programs.

Pending new project

Funding agency: NIH-NCI
Grant number: R01 CA93546
Fund amount: $175K/year
Funding period: 07/01/2003-06/30/2008
Title: Maintenance of Genetic Integrity in Mammalian Cells
Description: This is a new R01 application aimed to further characterize the functional role of BCCIP in DNA repair.

D7. Employment or research opportunities.

Not applicable.

E. Conclusions

We have shown that the C-terminal domain of human BRCA2 protein interacts with RAD51 protein, and that this domain is involved in the regulation of recombinational repair. In addition,this domain seems to be essential for cell growth control since overexpression of it results in inhibition of cell growth. We have also identified two new BRCA2-interacting proteins, BCCIP and filamin-1/ABP-280. These findings are potentially important to elucidate the mechanism by which BRCA2 suppresses breast cancer, and provide new insights to BRCA2's function. This project has resulted in 2 published, one submitted papers, and 9 presentations in national conferences. We anticipate at least one more paper will be submitted based on the work of this study.

F. References

1. Scully, R., Chen, J., Plug, A., Xiao, Y., Weaver, D., Feunteun, J., Ashley, T., and Livingston, D. M. Association of BRCA1 with Rad51 in mitotic and meiotic cells, Cell. *88:* 265-75, 1997.
2. Sharan, S. K., Morimatsu, M., Albrecht, U., Lim, D. S., Regel, E., Dinh, C., Sands, A., Eichele, G., Hasty, P., and Bradley, A. Embryonic lethality and radiation hypersensitivity mediated by Rad51 in mice lacking Brca2, Nature. *386:* 804-10, 1997.
3. Wong, A. K. C., Pero, R., Ormonde, P. A., Tavtigian, S. V., and Bartel, P. L. RAD51 interacts with the evolutionarily conserved BRC motifs in the human breast cancer susceptibility gene brca2, J Biol Chem. *272:* 31941-4, 1997.
4. Katagiri, T., Saito, H., Shinohara, A., Ogawa, H., Kamada, N., Nakamura, Y., and Miki, Y. Multiple possible sites of BRCA2 interacting with DNA repair protein RAD51, Genes Chromosomes Cancer. *21:* 217-22, 1998.
5. Chen, P. L., Chen, C. F., Chen, Y., Xiao, J., Sharp, Z. D., and Lee, W. H. The BRC repeats in BRCA2 are critical for RAD51 binding and resistance to methyl methanesulfonate treatment, Proc Natl Acad Sci U S A. *95:* 5287-92, 1998.
6. Zheng, L., Li, S., Boyer, T. G., and Lee, W. H. Lessons learned from BRCA1 and BRCA2, Oncogene. *19:* 6159-75, 2000.
7. Chen, C. F., Chen, P. L., Zhong, Q., Sharp, Z. D., and Lee, W. H. Expression of BRC repeats in breast cancer cells disrupts the BRCA2-Rad51 complex and leads to radiation hypersensitivity and loss of G(2)/M checkpoint control, J Biol Chem. *274:* 32931-5, 1999.
8. Xia, F., Taghian, D. G., DeFrank, J. S., Zeng, Z. C., Willers, H., Iliakis, G., and Powell, S. N. Deficiency of human BRCA2 leads to impaired homologous recombination but maintains normal nonhomologous end joining, Proc Natl Acad Sci U S A. *98:* 8644-9, 2001.

G. Appendices

1. Liu, J., Yuan, Y., Huan, J., and Shen, Z. 2001. Inhibition of brain and breast cancer cell growth by BCCIPα, an evolutionarily conserved nuclear protein that interacts with BRCA2. Oncogene, 20:336-345.
2. Yuan, Y., and Shen, Z. 2001. Interaction with BRCA2 suggests a role of filamin-A (hsFLNa) in DNA damage response. J. Biol. Chem. 276: 48318-48324.
3. Meng, X., Liu, J., Xu Guo, and Shen, Z. 2002. Genomic structure of the human BCCIP gene and its role in G1-S transition. Revision submitted to Oncogene.

Oncogene (2001) 20, 336–345

www.nature.com/onc

Inhibition of breast and brain cancer cell growth by BCCIPα, an evolutionarily conserved nuclear protein that interacts with BRCA2

Jingmei Liu[1], Yuan Yuan[1,2], Juan Huan[2] and Zhiyuan Shen*[,1]

[1]*Department of Molecular Genetics and Microbiology, University of New Mexico Health Sciences Center; 915 Camino de Salud, NE. Albuquerque, New Mexico, NM 87131, USA;* [2]*Graduate Program of Molecular Genetics, College of Medicine, University of Illinois at Chicago, 900 S. Ashland Ave. Chicago, Illinois, IL 60607, USA*

BRCA2 is a tumor suppressor gene involved in mammary tumorigenesis. Although important functions have been assigned to a few conserved domains of BRCA2, little is known about the longest internal conserved domain encoded by exons 14–24. We identified a novel protein, designated BCCIPα, that interacts with part of the internal conserved region of human BRCA2. Human BCCIP represents a family of proteins that are evolutionarily conserved, and contain three distinct domains: an N-terminus acidic domain (NAD) of 30–60 amino acids, an internal conserved domain (ICD) of 180–220 amino acids, and a C-terminus variable domain (CVD) of 30–60 amino acids. The N-terminal half of the human BCCIP ICD shares moderate homology with regions of calmodulin and M-calpain, suggesting that BCCIP may also bind Ca. Human cells express both a longer, BCCIPα, and a shorter, BCCIPβ, form of the protein, which differ in their CVD. BCCIP is a nuclear protein highly expressed in testis. Although BCCIPβ expression is relatively consistent in cancer cells, the expression of BCCIPα varies in cancer cell lines. The *BCCIPα* gene is located at chromosome 10q25.3–26.2, a region frequently altered in brain and other cancers. Furthermore, expression of BCCIPα inhibits breast and brain cancer cell growth, but fails to inhibit HT1080 cells and a non-transformed human skin fibroblast. These results suggest that BCCIPα is an important cofactor for BRCA2 in tumor suppression. *Oncogene* (2001) **20,** 336–345.

Keywords: BRCA2; calcium-binding protein; BCCIP

Introduction

The human tumor suppressor gene *BRCA2* encodes a large protein of 3418 amino acids. Mutations of *BRCA2* contribute to a significant portion of hereditary breast cancers. BRCA2 protein has no significant homology with any protein of known function. The overall homology between human and mouse BRCA2 is moderate at about 59%. Highly conserved regions (>75% homology) have been identified in human and mouse BRCA2. It is expected that important functions of BRCA2 reside in these conserved domains. Based on the functional analysis of the conserved BRCA2 domains, several models have been proposed for the role of BRCA2 in tumor suppression.

An N-terminus conserved domain in exon 3 (amino acids 48–105) has been implicated in transcriptional regulation of gene expression (Milner *et al.*, 1997; Nordling *et al.*, 1998). Deletion of this region has been identified in breast cancers (Nordling *et al.*, 1998). Therefore, the transcription activity itself is directly relevant to tumorigenesis.

Although the overall sequence in exon 11 shows only moderate homology between mouse and human BRCA2, eight internal BRC repeats in exon 11 are highly conserved (Bignell *et al.*, 1997). Each of the repeats is about 90 amino-acid long, and some of these repeats interact with RAD51 (Katagiri *et al.*, 1998; Marmorstein *et al.*, 1998; Wong *et al.*, 1997). A conserved C-terminal BRCA2 domain (amino acids 3196–3232 of mouse BRCA2) also mediates BRCA2/RAD51 interaction (Sharan *et al.*, 1997), and corresponds to a human BRCA2 C-terminus domain that is deleted in most truncating mutations of *BRCA2*. This region of mouse BRCA2 has 72% amino acid identity with human BRCA2. Functional analysis of these conserved domains in BRCA2 suggests that human BRCA2 may participate in RAD51-dependent DNA homologous recombination, thereby serving as a 'caretaker' of genome stability. Mutation of *BRCA2* that directly affects these RAD51-interaction domains could result in genomic instability, and promote tumorigenesis (Chen *et al.*, 1999; Yuan *et al.*, 1999).

A third model involves the cellular localization of BRCA2 proteins. The functional nuclear localization signals (NLS) for BRCA2 have been identified near the C-terminus (Spain *et al.*, 1999; Yano *et al.*, 2000). Most of the BRCA2 mutations identified in breast cancers are truncations, resulting in deletion of the C-terminal NLS. It is possible that the lack of NLS in BRCA2 mutants results in abnormal cellular localization of BRCA2, preventing BRCA2 function (such as transcription and genome stability control), and subsequently responsible for tumorigenesis associated with BRCA2 mutation. This model may explain cases that involve the deletion of NLS in BRCA2 patients. However, some internal mutations, as exemplified by deletion of the transcriptional domain (Koul *et al.*,

*Correspondence: Z Shen
Received 16 August 2000; revised 8 November 2000; accepted 9 November 2000

1999), would not affect the cellular location of BRCA2. They may still be responsible for tumorigenesis.

BRCA2 may be a protein with multiple functional domains. Another highly conserved region precedes the C-terminus RAD51-interaction domain. This domain is the longest conserved domain in BRCA2. It covers exons 14–24 (Gayther and Ponder, 1998). The role of this region in tumorigenesis is unclear. It is anticipated that this conserved domain carries essential, yet to be identified, functions of BRCA2. It may possess cellular functions other than RAD51-associated DNA homologous recombination. Identification of novel proteins associating with BRCA2 would provide clues for additional *BRCA2* functions. Using part of the long internal conserved domain covering exon 14–24 as 'bait' in a yeast two-hybrid screen, we identified a novel nuclear protein, designated BCCIPα that interacts with a part of this conserved region.

Results and discussion

Identification of a BRCA2-interacting protein, BCCIPα

Amino acids 2883–3053 of BRCA2 (termed BRCA2H) forms the longest internal conserved region encoded by exons 14–24. BRCA2H is 78% identical between mouse and human, compared to the overall homology of 59%. Using Gal4-DB/BRCA2H as 'bait' in a yeast two-hybrid assay, we screened 4×10^5 independent clones of a human cDNA library, and identified 14 interacting clones. DNA sequencing identified five clones that were derived from the same gene. Clone number 5 contained the longest cDNA, and encoded an open reading frame with a stop codon at the 3′-end, but no translation start codon at the 5′-end. This gene was assigned the symbol of *BCCIP* by the HUGO Gene Nomenclature Committee.

The sequence of our BCCIP cDNA was compared to databases of human EST. From the resulting analysis, we concluded that our clone was missing 42 nucleotides from the 5′-end. In addition, we discovered that some BCCIP cDNA have different 3′-end. The two types of cDNA encode protein of either 322 or 314 amino acids, and designated BCCIPα and BCCIPβ. BCCIPα and BCCIPβ have identical amino acids N-terminus 258 amino acids, but differ in their C-terminus (Figure 1a).

Further analysis showed that amino acids 45–100 of BCCIP shares 29% identity and 58% similarity to the Ca-binding domain of M-calpain (Figure 1b) (Pontremoli *et al.*, 1999). The same region also shares homology with the N-terminus Ca-binding site of calmodulin. Calmodulin is composed of three distinct domains (Yjandra *et al.*, 1999), an N-terminus calcium binding domain, a C-terminus calcium-binding domain, and an internal helix domain. In addition to the Ca-binding site, amino acids 100–150 of human BCCIP also share homology with the internal helix of calmodulin. Amino acids 50–150 of human BCCIP shares 26% identity and 45% similarity with amino acids 1–90 of the calcium binding regulator protein calmodulin (Yjandra *et al.*, 1999) (Figure 1b). Therefore, BCCIP is a putative Ca-binding protein.

Finally, we identified BCCIP-homologous genes from *C. elegans*, *S. cerevisiae*, and *A. thaliana*. Their anticipated protein sequences share a common structural profile with human BCCIPα and BCCIPβ. All have an N-terminus acidic domain (NAD) rich in residues DE (aspartate and glutamate), an internal conserved domain (ICD), and a C-terminus variable domain (CVD) (Figure 2a).

The DE-rich NAD domain shares moderate homology with many proteins having acidic domains. The CVD shares no homology among BCCIP family members, except that mouse BCCIP and human BCCIPβ are ~70% identical. The ICD is evolutionary conserved among the species analysed. For example, human and mouse BCCIP share 97% similarity, while the yeast and plant BCCIP share about 70% similarity to human BCCIP (Figure 2a). The putative Ca-binding domain resides in the ICD (Figure 2b).

In vivo *interaction between BCCIPα and BRCA2*

In order to confirm the complex formation between BRCA2 and BCCIP *in vivo*, the proteins were expressed in 293 human kidney cells, and co-immunoprecipitation experiments were performed.

In the first experiment, HA-tagged BRCA2 fragments BRCA2F (amino acids 2883–3418) and BRCA2B (amino acids 2883–3194) were co-expressed with Flag-tagged BCCIPα in 293 cells. The HA-tagged BRCA2 proteins were precipitated with an anti-HA affinity matrix, and co-precipitated Flag-BCCIPα was detected by anti BCCIP antibodies. As demonstrated in Figure 3a, HA-tag alone (negative control) did not precipitate BCCIPα (Figure 3a, lane 4). However, BCCIPα was co-precipitated with both HA-BRCA2F and HA-BRCA2B (Figure 3a, lanes 5 and 6), suggesting that full-length BCCIPα interacts with the BRCA2.

In a second experiment, HA-tagged BCCIPα, UBC9, and RAD51 proteins were transiently expressed in 293 cells, and immunoprecipitated with the anti-HA affinity matrix. The precipitated HA-tagged proteins were detected with anti-HA tag (lower panel of Figure 3b). Co-immunoprecipitated endogenous BRCA2 proteins were detected by rabbit anti-BRCA2 antibodies (upper panel of Figure 3b). As demonstrated in the top panel of Figure 3b (lane 8), endogenous BRCA2 protein was precipitated with HA-RAD51 as previously demonstrated (Marmorstein *et al.*, 1998; Tan *et al.*, 1999), and HA-tag (Figure 3b, top panel, lane 5) and HA-UBC9 (Figure 3b, top panel, lane 7) did not precipitate BRCA2. However, HA-BCCIPα co-precipitated BRCA2. These data suggest a stable complex formation between full-length BRCA2 and BCCIPα in human cells.

A

```
Amino Acid Sequences of BCCIPα and BCCIPβ.

BCCIPα    MASRSKRRAVESGVPQPPDPPVQRDEEEEKEVENEDEDDD     40
          |||||||||||||||||||||||||||||||||||||||||
BCCIPβ    MASRSKRRAVESGVPQPPDPPVQRDEEEEKEVENEDEDDD     40

BCCIPα    DSDKEKDEEDEVIDEEVNIEFEAYSLSDNDYDGIKKLLQQ     80
          ||||||||||||||||||||||||||||||||||||||||
BCCIPβ    DSDKEKDEEDEVIDEEVNIEFEAYSLSDNDYDGIKKLLQQ     80

BCCIPα    LFLKAPVNTAELTDLLIQQNHIGSVIKQTDVSEDSNDDMD     120
          ||||||||||||||||||||||||||||||||||||||||
BCCIPβ    LFLKAPVNTAELTDLLIQQNHIGSVIKQTDVSEDSNDDMD     120

BCCIPα    EDEVFGFISLLNLTERKGTQCVEQIQELVLRFCEKNCEKS     160
          ||||||||||||||||||||||||||||||||||||||||
BCCIPβ    EDEVFGFISLLNLTERKGTQCVEQIQELVLRFCEKNCEKS     160

BCCIPα    MVEQLDKFLNDTTKPVGLLLSERFINVPPQIALPMYQQLQ     200
          ||||||||||||||||||||||||||||||||||||||||
BCCIPβ    MVEQLDKFLNDTTKPVGLLLSERFINVPPQIALPMYQQLQ     200

BCCIPα    KELAGAHRTNKPCGKCYFYLLISKTFVEAGKNNSKKKPSN     240
          ||||||||||||||||||||||||||||||||||||||||
BCCIPβ    KELAGAHRTNKPCGKCYFYLLISKTFVEAGKNNSKKKPSN     240

BCCIPα    KKKAALMFANAEEEFFYEEQGKPE.........VLGGPD     270
          ||||||||||||||||||                |||
BCCIPβ    KKKAALMFANAEEEFFYEkailkfnysvqeesdtcLGGkw     280

BCCIPα    TRRGLEPVPIQHNGGSRGQ..VTALVSLKAGLIQSRSTLS     308
                |     |      ||  |
BCCIPβ    sfddvpmtPlrtvmlipGdkmneimdkLKeyLsv.....     314

BCCIPα    DFQGTFMTVGIALS                               322
BCCIPβ    ..............                               314
```

B

```
     v70       v80       v90       v100      v110      v120      v130      v140
LSDNDYDGIKKLLQQLFLKAPVNTAELTDLLIQQNHIGSVIKQTDVSEDSND-DMDEDEVFGFISLLNLTER--KGTQCVEQIQE  BCCIP
L:::: ..:K. :  LF K.  .T . .:L .  . :G   .:::: :  N: D D.:.::F .:L.: .R  K:T:. E:I:E
LTEEQIAEFKEAFS-LFDKDGDGTITTKELGTVMRSLGQNPTEAELQDMINEVDADGNGTIDFPEFLTMMARKMKDTDSEEEIRE  Calmodulin
     ^10       ^20       ^30       ^40       ^50       ^60       ^70       ^80

     v50       v60       v70       v80       v90
EKDEEDEVIDEEVNIEFEAYSLSDNDY-DGIKKLLQQLF-LKAPVNTAELTDLL   BCCIP
EK..: :.:D:E:: ::E.:.:S::D  DG:::L:.QL   .A ::: EL .:L
EKKADYQAVDDEIEANLEEFDISEDDIDDGVRRLFAQLAGEDAEISAFELQTIL   M-calpain
      ^510      ^520      ^530      ^540      ^550
```

Figure 1 Amino acid sequence analysis of BCCIP proteins. (**a**) Comparison of amino acid sequences between BCCIPα and BCCIPβ. BCCIPα and BCCIPβ share an identical 258 amino acid sequence at their N-terminus, but vary in their C-terminus amino acid sequences. (**b**) Sequence comparison of BCCIP with the Ca-binding regions of calmodulin and M-calpain. The top panel is an amino acid alignment of BCCIP with human calmodulin. The bottom panel is an amino acid alignment of BCCIP with human M-calpain. The numbers indicate the amino acid residue number from the N-terminus of each protein

A small region of BRCA2 is responsible for BCCIP interaction

To further characterize the interaction between BCCIPα and BRCA2, we fused a series of BRCA2 fragments with the Gal4-DNA binding domain, and tested their interaction with Gal4-DNA activation domain fused BCCIPα protein using LacZ as reporter in the independent yeast strain SF526. As shown in Figure 4a, BRCA2H undoubtedly interacts with BCCIP; the minimum interacting region of BRCA2 is in amino acids 2973–3001.

To confirm this, a set of GST-fusion proteins of BRCA2 fragments was purified. GST-BRCA2 proteins were incubated with His-BCCIPα protein, and pulled down with glutathion beads. Bound His-BCCIPα proteins were analysed with Western blot. As shown in Figure 4b, GST protein and resin alone could not pull down His-BCCIPα. However, BRCA2 proteins containing region 2973–3001 pulled down His-BCCIPα, suggesting an interaction between His-BCCIPα and this BRCA2 region. This region is 71% identical between mouse and human BRCA2, significantly above the average homology between human and mouse BRCA2. Since purified proteins were used for the binding assay, this demonstrates that BRCA2 and BCCIPα form a direct protein–protein interaction.

Recombinant BCCIPα protein, BCCIP antibodies, and expression of BCCIP in human tissues

We subcloned the BCCIPα into pET28 and purified His tagged BCCIP recombinant protein from bacteria (Figure 5a, lane 2). GST tagged BCCIPα proteins were also purified (Figure 5a, lane 3). The His-BCCIPα was used to make rabbit polyclonal antibodies against BCCIP, and GST-BCCIPα was used to affinity purify

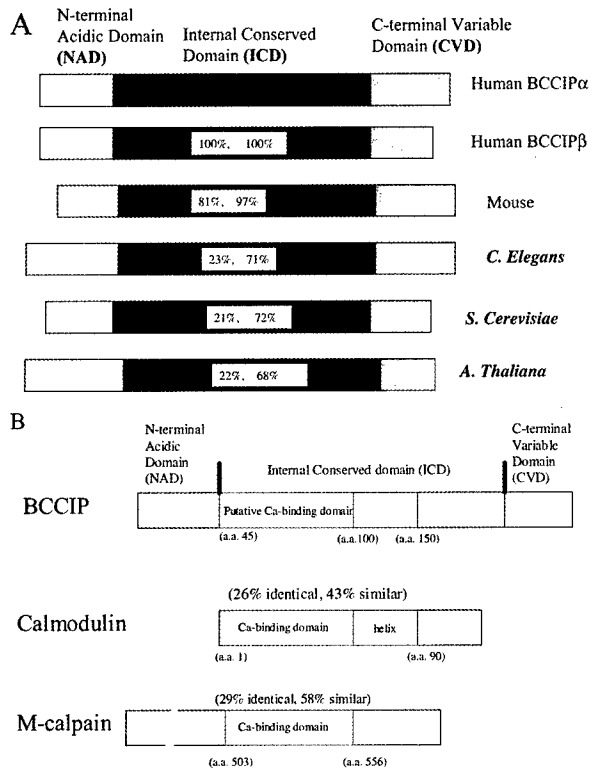

Figure 2 Domain analysis of BCCIP proteins (drawing not to scale). (**a**) Domain comparison of human BCCIP with its homologues in other species. According to the sequence conservation, the human BCCIP was arbitrarily divided into three domains: an N-terminus Acidic Domain (NAD), an Internal Conserved Domain (ICD), and a C-terminus Variable Domain (CVD). Numbers in the ICD of BCCIPs indicate the percentages of sequence identity and similarity of the specific BCCIP with human BCCIPα. (**b**) Sequence similarity of the putative Ca-binding domain in the internal conserved domain (ICD) of human BCCIP with human calmodulin and the a region of M-Calpain. Numbers in the parenthesis above the Ca-binding domains of calmodulin and M-calpain indicate their percentage of sequence identity and similarity to the putative Ca-binding site of human BCCIP

the anti-BCCIP antibodies. These antibodies recognized the full-length BCCIPα, as well as the N-terminal common region between BCCIPα and BCCIPβ (data not shown). Therefore the polyclonal anti-BCCIPα antibodies also recognize BCCIPβ.

These antibodies are reactive to two species of proteins from human skin fibroblasts (HSF) and HT1080 fibrosarcoma cells (Figure 5b). Since BCCIPα shares significant homology to BCCIPβ, and the antibodies recognize the N-terminus common region of BCCIPα and BCCIPβ, we predict that the top band (~50 kDa) is BCCIPα (322 amino acids), and the lower band (~46 kDA) is BCCIPβ (314 amino acids).

A human tissue protein membrane was purchased from DNA Technology Inc. Although the resolution of the pre-made membrane was compromised, and it is hard to distinguish the bands for BCCIPα and BCCIPβ in tissues (Figure 5c), it is interesting that the BCCIP proteins are highly expressed in testis, as are BRCA2

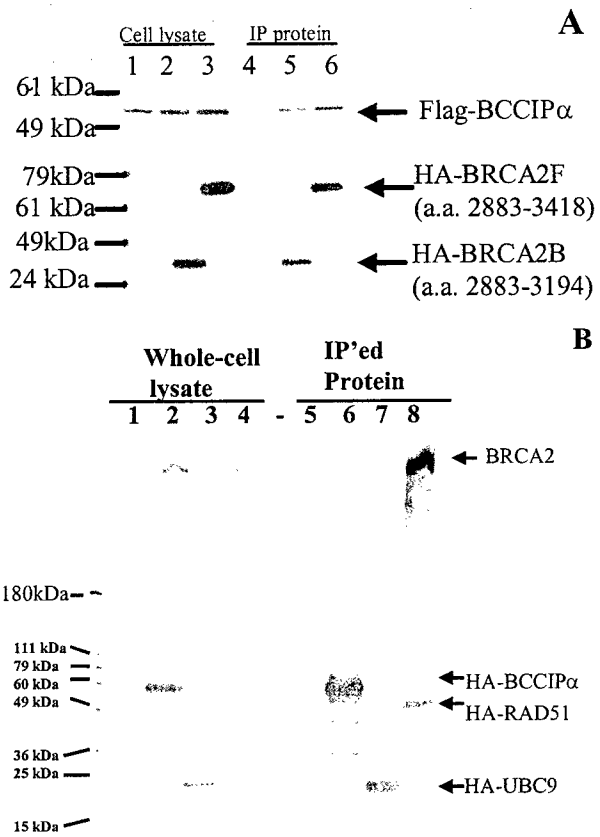

Figure 3 *In vivo* protein complex formation between BRCA2 and BCCIPα. (**a**) Co-immunoprecipitation of BCCIPα with BRCA2 fragments. Lanes 1–3 are whole cell protein extracts from 293 cells transfected with various plasmids. Lanes 4–6 are the anti-HA matrix precipitated proteins from the whole cell extracts. Lanes 1 and 4 were derived from co-expression of Flag-BCCIPα and a control vector (pHA-CMV), lanes 2 and 5 were derived from co-expression of Flag-BCCIPα and HA-BRCA2B (amino acid 2883–3149), and lanes 3 and 6 are extracts from cells expressing Flag-BCCIPα and HA-BRCA2F (amino acid 2883–3418). The bottom panel is blotted with anti-HA antibodies, demonstrating that HA-BRCA2B and HA-BRCA2F are expressed in the total cells extracts (lanes 2 and 3), and were precipitated with anti-HA matrix (lanes 4 and 5). The top panel was blotted with anti-BCCIP antibodies, demonstrating that BCCIPα can be co-precipitated with the HA-BRCA2 and BRCA2F (lanes 5 and 6). This data suggest that a C-terminus of BRCA2 region containing amino acids 2883–3149 forms a complex with full-length BCCIPα. (**b**) Co-immunoprecipitation of endogenous BRCA2 from 293 cells with HA-BCCIPα. Lanes 1–4 are whole cell protein extracts (5 μg of each) from cells that were transfected with pHA-CMV (lane 1), pHA-CMV/BCCIPα (lane 2), pHA-CMV/UBC9 (lane 3), and pHA-CMV/RAD51 (lane 4). Lanes 5, 6, 7 and 8 are Anti-HA resin precipitated proteins from whole cell extract as in lanes 1, 2, 3 and 4 respectively. The bottom panel is blotted with anti-HA antibodies, showing that the HA-BCCIPα (lanes 2 and 6), HA-UBC9 (lanes 3 and 7), and HA-RAD51 (lanes 4 and 8) are expressed in transfected cells (lanes 2, 3 and 4) and precipitated with anti-HA matrix (lanes 6, 7 and 8). The top panel demonstrates that the endogenous BRCA2 protein exists in 293 cells transfected with control vector (lane 1), pHA-CMV/BCCIP (lane 2), pHA-CMV/UBC9 (lane 3) and pHA-CMV/RAD51 (lane 4), but was only co-precipitated when HA-BCCIP (lane 6) or HA-RAD51 (lane 8) was expressed. This data suggest a stable complex can be formed between the full-length endogenous BRCA2 and full-length BCCIP protein

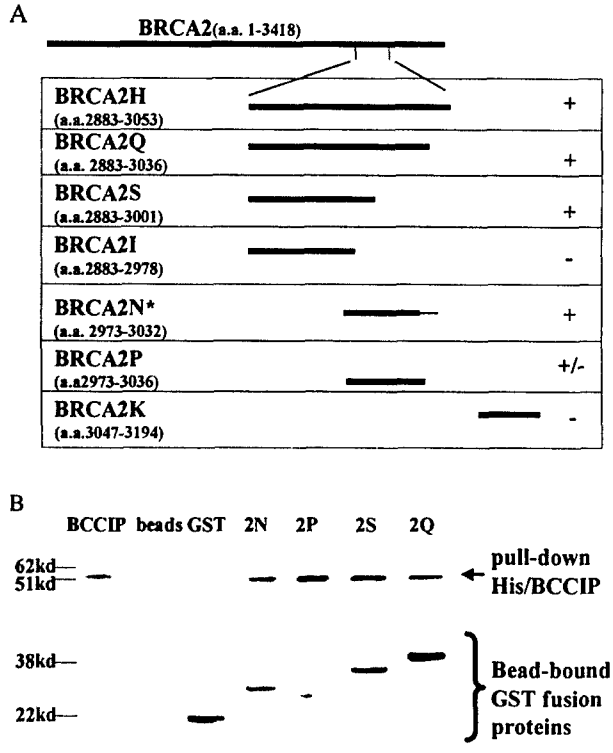

Figure 4 Mapping of BRCA2 regions that interact with BCCIP. (**a**) Results from two-hybrid analysis. '+' on the right side of the illustration indicates a positive interaction of the BRCA2 fragment (left side) with BCCIPα in yeast two-hybrid system (drawing not to scale). The amino acid border of various BRCA2 fragments are listed in the parenthesis under the name of the BRCA2 fragment. (**b**) His-BCCIPα protein that was co-precipitated with GST BRCA2 fusion proteins. Lane 'BCCIP' indicates the purified His-BCIPPα protein loaded as positive control for Western blot. Lane 'beads' is loaded with co-precipitated His-BCCIPα protein with glutathion beads. The rest lanes are the co-precipitated His-BCCIP proteins with GST or GST fusion proteins as labeled on the top of the panel. The same BRCA2 fragment nomenclature as (**a**) is used in this figure

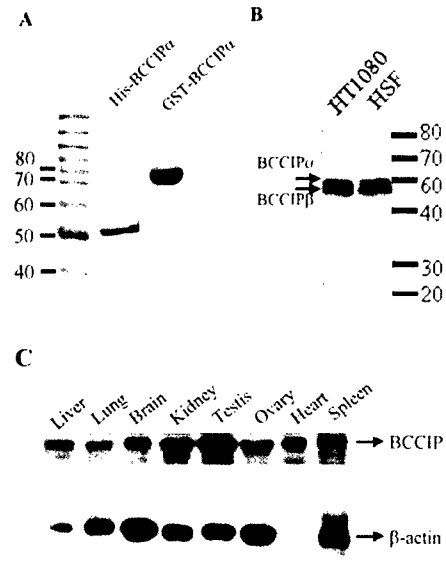

Figure 5 BCCIPα recombinant proteins, antibodies, and BCCIP protein expression in human tissues. (**a**) Commassie stained His-tagged BCCIPα and GST-tagged BCCIPα recombinant proteins that were used for polyclonal antibody production in rabbit and affinity purification. Numbers on the left indicate the locations of standard protein markers with corresponding size (kDa). (**b**) Two distinctive species of BCCIP are reactive to BCCIP antibodies in normal human skin fibroblasts (HSF), and HT1080 cells. The higher molecular weight band is designated BCCIPα (approximately 50 kDa), and the lower molecular weight band is designated BCCIPβ (approximately 46 kDa). Numbers on the right indicate the locations of standard protein markers with corresponding size (kDa). (**c**) BCCIPs are expressed in several human tissues, with the highest expression level in testis. The double-band pattern is not readily visible in the tissues in this illustration due to the compromised resolution of the pre-made membrane provided by DNA Technology. However, the same double-band pattern, as in (**b**), was observed with a lighter exposure (data not shown) in all the tissues

(Sharan and Bradley, 1997) and RAD51 (Shinohara *et al.*, 1993).

Nuclear localization of BCCIP

To determine the cellular localization of BCCIP, we stained the breast cancer cell line MCF-7 with the affinity purified polyclonal BCCIP antibodies. As shown in Figure 6, BCCIP proteins are predominantly expressed in the nucleus. Under the same condition, pre-immuno serum did not react with the nucleus (data not shown). It is interesting that BCCIP reactive proteins do not colocalize with condensed chromosome DNA during mitosis (Figure 6a,c). Confocal microscopy of HeLa cells and human skin fibroblasts showed the same cellular distribution as MCF-7 cells (data not shown). We also expressed EGFP-tagged BCCIPα protein in HeLa cells, confirming that the majority of the BCCIPα protein localizes to the nucleus (data not shown).

BCCIPα *is located on chromosome 10 at q25.3–26.2*

We used *BCCIPα* cDNA as a probe for a FISH analysis. Among 100 mitotic cells analysed, 67 of them have paired FISH signals, and all of them were present near the end of chromosome 10q (Figure 7a). Further analysis mapped this gene to 10q25.3–26.2 (Figure 7b). To confirm this finding, we used the BCCIP sequence as probe to search a human chromosome marker database, and identified a marker (SGC33832) at chromosome 10q26.1. This marker has identical sequence to part of the BCCIPα cDNA. Therefore, this result confirmed that *BCCIPα* is present at 10q25.3–26.2, and is likely centered at 10q26.1.

Abnormalities in regions of chromosome 10q25.2–26.2 have been observed in many tumors, including brain tumors (Maier *et al.*, 1997; Rasheed *et al.*, 1995), endometrial tumors (Peiffer *et al.*, 1995), lung cancers (Kim *et al.*, 1998; Petersen *et al.*, 1998), melanoma (Robertson *et al.*, 1999; Walker *et al.*, 1995), and other tumors (Ittmann, 1996). It has also been reported that the deletion of this region is responsible for develop-

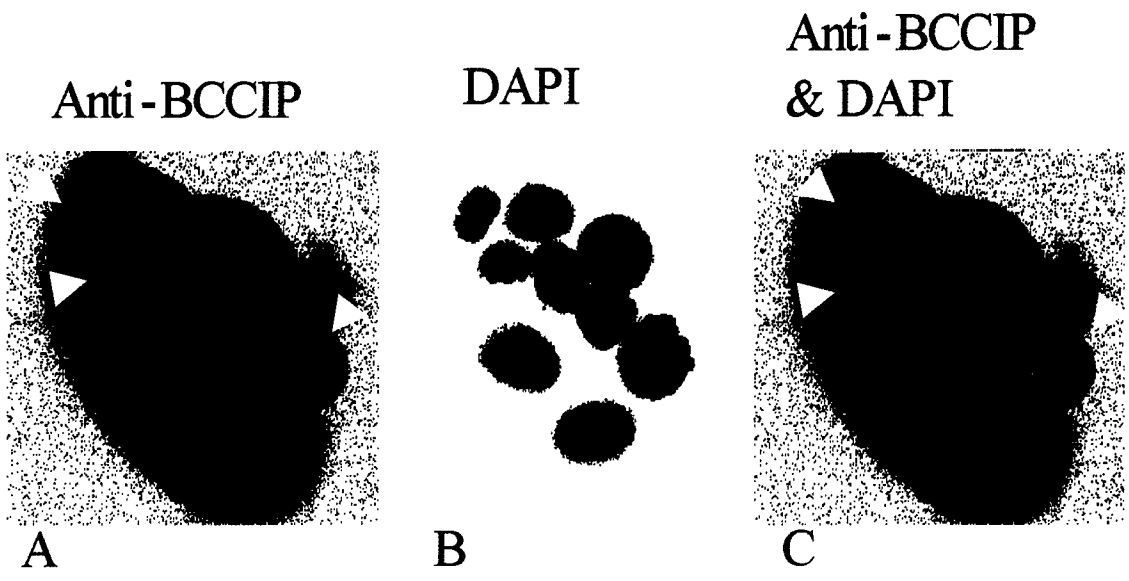

Figure 6 BCCIP localizes to nucleus in MCF-7 breast cancer cells. Shown in the figure is a cluster of nine MCF-9 cells. Affinity purified polyclonal anti-BCCIP antibodies were used for the immunostaining. Red signals from (**a**) are the anti-BCCIP antibody reactive proteins. Three mitotic cells with condensed DNA are indicated by arrows. The blue signals from (**b**) are DAPI stained cellular DNA, showing the nucleus and/or condensed chromosome DNA (arrows). (**c**) Shows both the DNA signal and BCCIP signals

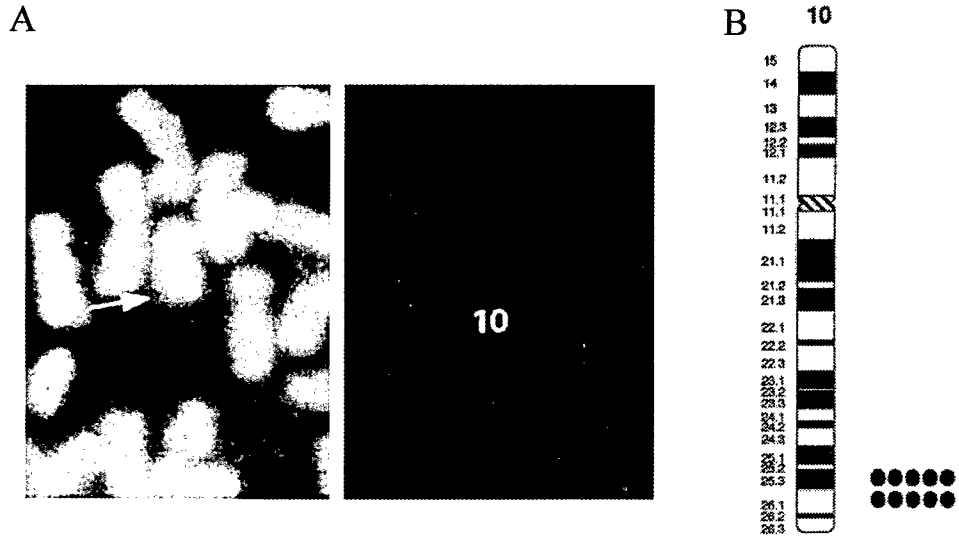

Figure 7 Chromosome location of *BCCIPα* gene. (**a**) FISH analysis of *BCCIPα* cDNA. The bright signal (arrow on the left panel) indicates the location of the BCCIP gene. The right panel is DAPI staining of the same mitotic cell showing chromosome 10. (**b**) The defined location of BCCIP on chromosome 10q25.3–26.2 (results from detailed band analysis of 10 individual cells)

mental retardation in children (Tanabe *et al*., 1999; Taysi *et al*., 1982; Waggoner *et al*., 1999).

At least one tumor suppressor is located in 10q25.3–26.2 (Petersen *et al*., 1998; Rasheed and Bigner, 1991; Rasheed *et al*., 1995). This tumor suppressor has been suggested to be responsible for brain tumors. A candidate tumor suppressor (DMBT1) was identified in this region (Mollenhauer *et al*., 1997). However, studies have shown that the status of DMBT1 in brain tumors has no connection with tumor phenotypes, suggesting that another gene in the region is responsible for brain tumors (Steck *et al*., 1999).

Expression of BCCIP proteins in cancer cells

To evaluate a possible association of BCCIP with human cancers, we examined BCCIPα and BCCIPβ expression in a number of cancer cell lines. As shown in Figure 8, the expression level of BCCIPβ is

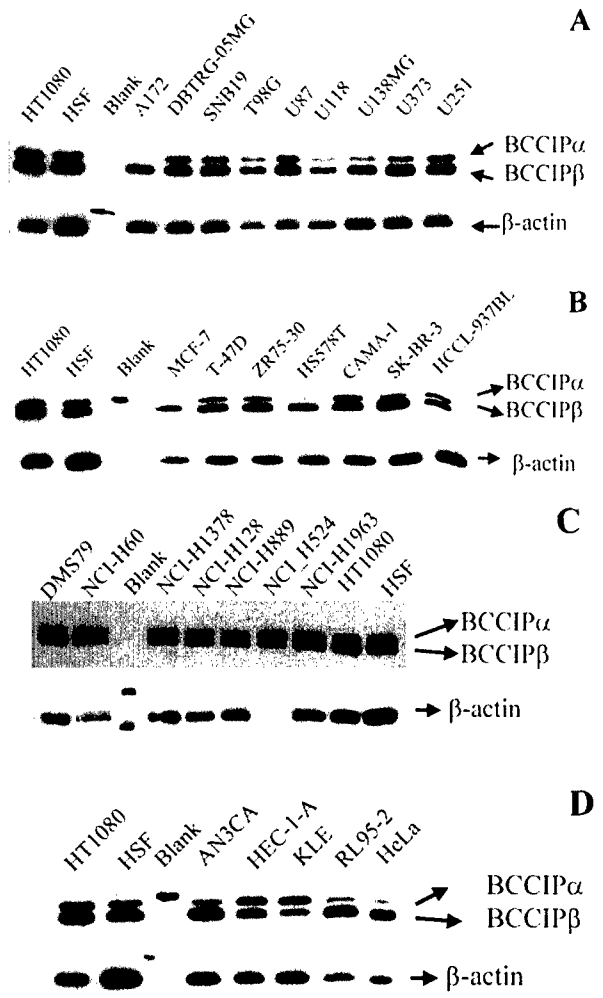

Figure 8 Expressions of BCCIPα and BCCIPβ in tumor cell lines. Five μg of total cell proteins were loaded on a 4–20% gradient SDS–PAGE gel, and immunoblotted with affinity purified anti-BCCIP antibodies (top panels), and then re-blotted with anti-actin antibodies (bottom panels). The labels on the top of each figure indicate specific cell lines. In each figure, HSF and HT1080 cell proteins were loaded to normalize the signals among the different immunoblot membranes. (**a**) Contains brain tumor cell lines, (**b**) for breast cancer cells, (**c**) for lung cancers, and (**d**) for endometrial tumor cells

relatively constant among these tumor cells, as compared to the protein level of β-actin. However, the level of BCCIPα varies significantly as compared to β-actin or BCCIPβ. Among the nine brain tumor cell lines (Figure 8a), A172 cells completely lack detectable BCCIPα expression, and U138MG and U118 showed reduced BCCIPα expression. Among the seven breast cancer cell lines (Figure 8b), MCF-7, SK-BR-3, and HS578T showed reduced BCCIPα expression. In the four cases of endometrial tumor cells (Figure 8d), two cell lines showed reduced BCCIPα levels, and two showed increased levels. However, the relative BCCIPα and BCCIPβ expression level was relatively consistent among the seven tested lung cancer cell lines (Figure 8c).

Inhibition of breast cancer cell growth by BCCIPα

We further expressed HA-tagged BCCIPα protein in a few brain and breast cancer cell lines. As demonstrated in Figure 9, expression of HA-BCCIPα caused no significant cell growth delay in normal human skin fibroblast (HSF) or in HT1080 fibrosarcoma cells. However, when the same control vector virus and HA-BCCIPα virus were used to infect brain and breast cancer cell lines, the HA-BCCIPα caused a growth delay. As shown by the growth curve of infected HSF, HT1080, A172, and MCF7 cells (Figure 10a–d), HA-BCCIPα inhibited the growth of MCF7 and A172, but not HSF and HT1080. As shown in Figure 10e, the levels of exogenously expressed HA-BCCIPα in MCF7, A172, HT1080 or HSF are comparable to the endogenous levels of BCCIP. These data conclude that expression of BCCIPα inhibits the growth of some breast cancer and brain tumor cells.

Considering the interaction of BCCIP with known tumor suppressor BRCA2, the similar tissue expression pattern of BCCIP with BRCA2, the *BCCIP* chromosome location to a region that is frequently altered in various tumors, the reduced or lacking of BCCIPα expression in tumor cells, and the inhibition of tumor cell growth, it is conceivable to suggest that *BCCIP* might be a candidate tumor suppressor for breast and brain tumors. However, more extensive studies are required to test this hypothesis. These will include at least, but not limited to, the following studies: extensive expression and mutation analysis of BCCIP in primary tumor specimens, suppression of tumor phenotypes in tumor cells by introducing wild type BCCIP into tumor cells with

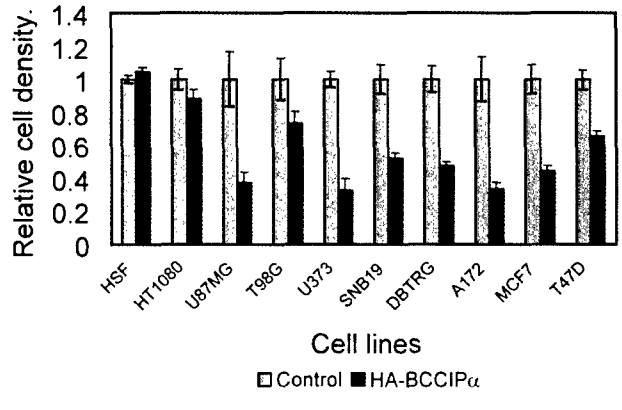

Figure 9 Inhibition of brain and breast cancer cell growth by expression of BCCIPα. Six brain tumor cell lines (U87MG, T98G, U373, SNB19, DGTRG and A172), two breast cancer cells (MCF7 and T47D), HT1080, and non-transformed HSF cells were plated in 6-well plates at 0.1×10^6 cells/ml. Eighteen hours after the plating, the cells were infected with virus that expresses HA-BCCIPα protein. Infected cells were selected by puromycin for 48 h, and allowed to grow for an additional 3 days. Cells were then counted. Shown in the figures are the relative numbers of cells for each cell line, normalized to the cells infected with control vectors

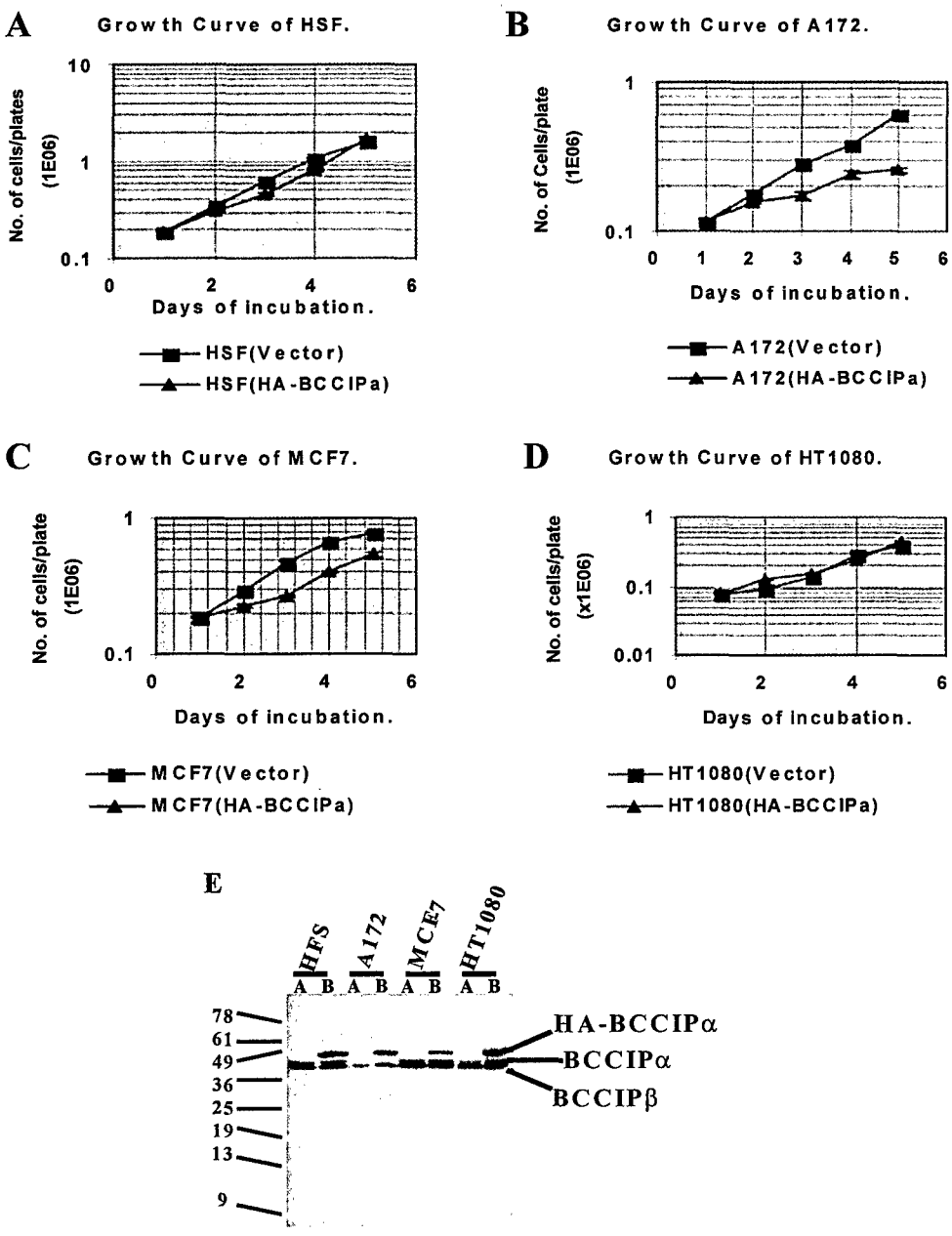

Figure 10 Growth inhibition of MCF7 breast cancer cells and A172 brain tumor cells by expression of HA-BCCIPα. The growth curves for HSF (**a**), A172 (**b**), MCF7 (**c**), and HT1080 (**d**) cells express HA-BCCIPα are compared with those of control cells. The representations of each marker are shown inside each panel of figures. (**e**) Is the immunoblot of the cells infected with control vector (lane A), or HA-BCCIPα (lane B) using anti-BCCIP antibodies. The exogenously expressed HA-BCCIPα is indicated on the right side of Figure 1e. As shown in this figure, the levels of exogenously expressed HA-BCCIPα are at about the same levels of endogenous BCCIPα or BCCIPβ in each of the cell lines. Numbers on the left are the locations of molecular weight markers (kDa). The specific cells used for the immunoblot are labeled on the top of the figure

BCCIP mutation, and promotion of tumorigenesis/carcinogenesis by inhibition of BCCIP gene function in normal cells.

Searching the yeast genome database, we have identified a yeast strain that has the *BCCIP* open reading frame deleted. It is interesting that the *BCCIP* null mutation is lethal to yeast, suggesting an essential role for *BCCIP* in yeast. Further analysis of the yeast *BCCIP* mutant will be performed to provide clues to human BCCIP function.

To summarize, we identified a new protein, designed BCCIP that interacts with BRCA2. At least two isoforms of this protein are expressed in human tissues. BCCIP is evolutionarily conserved with several distinctive structural domains. A part of the internal conserved domain of BCCIP shares a moderate degree of homology with the a region of M-calpain and

calmodulin. BCCIPα inhibits brain and breast cancer cell growth. Further studies will be focused on its expression in human tumors and its functional role in tumorigenesis.

Materials and methods

Plasmids

A fragment of BRCA2 cDNA covering exons 21–24 was isolated using RT–PCR, and confirmed by sequencing. This fragment was linked with *Bam*HI and *Sal*I sites, and fused to the Gal4-binding domain in the yeast two-hybrid vector pAS2-1, resulting in pAS2-1/BRCA2H. PCR primers tagged with *Bam*HI/*Sal*I sites were used to amplify regions of BRCA2 cDNA, and cloned into pGEX-5X (Pharmacia) to generate vectors that express glutathion S-transferase (GST) fused protein fragments of BRCA2. The same regions of BRCA2 were also cloned into the two-hybrid vector pGBT9, resulting pGBT9/BRCA2H, to express Gal4-DNA binding domain fused protein in yeast. BCCIPα cDNA was cloned into pET28 (Novagen), creating pET28/BCCIPα, which expresses histidine tagged BCCIPα protein in BL21 (DE3) cells. BCCIP cDNA was also cloned into pGEX-5x to generate pGEX/BCCIP, which expresses recombinant GST-BCCIP fusion protein in BL21 cells. All plasmid constructs were confirmed by DNA sequencing. Plasmids that express HA-UBC9 and HA-RAD51 are described as before (Li *et al*., 2000).

Recombinant proteins and BCCIP antibodies

Recombinant protein expression and purification were performed as previously described (Shen *et al*., 1996b). Briefly, pET28/BCCIPα was transfected into BL21(DE3) cells, and the $(His)_6$-tagged BCCIP protein (His-BCCIPα) was expressed and purified. GST-BCCIPα and GST-BRCA2 fusion proteins were expressed and purified in BL21 cells using pGEX/BCCIPα, and pGEX/BRCA2 vectors. His-BCCIPα was injected into rabbits to produce polyclonal antibodies, and GST-BCCIPα was used for affinity purification of polyclonal anti-BCCIP antibodies.

BCCIPα DNA sequence and human EST database analysis

Plasmids from positive clones of the two-hybrid screen were sequenced and data were analysed with DNA Star sequence analysis software. The GenBank nucleic acid and human EST databases were searched to identify matching ESTs. The complete cDNA sequence of BCCIPα was constructed from the cDNA sequence of our clones and matching ESTs.

Protein interaction assays

pAS2-1/BRCA2H was used to screen a cDNA library expressing Gal4-DNA activation domain fused proteins (Clonetech, Palo Alto, CA, USA) as described (Shen *et al*., 1996a). MV103 cells hosting LacZ and Uracil, and Histidine reporters were used for the screen (Vidal, 1997). To confirm the two-hybrid interaction, an independent two-hybrid assay and *in vitro* GST pull-down assays were performed as described (Shen *et al*., 1996b). Briefly, various regions of BRCA2 cDNA were cloned into pGBT9. These vectors were co-transfected with pACT/BCCIPα, and assayed for LacZ activity in the host cell strain SFY526 (Clontech, Palo Alto, CA, USA). GST-tagged BRCA2 fragments were bound to glutathione beads and incubated with His-tagged BCCIP protein. After extensive washing, His-BCCIPα proteins bound to GST-fusion proteins were analysed by Western blot using anti-BCCIP antibodies.

Immunoprecipitation and immunoblotting

Cultured human cells were collected, treated with lysis buffer (150 mM NaCl, 1 mM EDTA, 50 mM Tris Cl, pH 7.5, 1% NP-40) for 30 min in ice, and sonicated, resulting in whole-cell extract. One mg of whole-cell extract was incubated with 50 μl of anti-HA Affinity Matrix (Roche Molecular Biochemicals) at 4°C on a rocker for 2 h. The matrix was washed six times in 1 ml of cold lysis buffer. Proteins bound to the beads were eluted in 2 × SDS sample buffer by boiling for 5 min, then resolved by SDS–PAGE and transferred to PVDF membrane (Osmonics). Immunoblotting using appropriate antibodies was as described before (Li *et al*., 2000). To detect BRCA2, a rabbit anti-BRCA2 antibody (Oncogene Researcher Products) was used.

Immunostaining and confocal microscopy

Cells were cultured on a cover slip, and fixed with cold 3% paraformaldehyde solution buffered with PBS for 1 h. Fixed slides were treated with permeabilization buffer (0.5% Triton X-100, 50 mM NaCl, 3 mM $MgCl_2$, 300 mM sucrose, and 20 mM HEPES, pH 7.4) for 20 min. Slides were blocked with 2% BSA in PBS for 30 min at room temperature, and incubated with 1 μg/ml of primary anti-BCCIP antibodies overnight at 4°C. After the primary antibody incubation, the slides were washed five times with PBS, and incubated with rhodamin-conjugated anti-rabbit IgG antibodies (Pierce) for 30 min at room temperature. Slides were washed with PBS five times, and mounted with Vectashield mounting solution containing 4′,6-diamidino-2-phenylindole (DAPI, Vector Laboratories, Burlingame, CA, USA). The slides were stored in the dark at 4°C. A Zeiss LSM510 confocal microscope with Ar/Kr and UV laser sources was used to observe the stained slides, and images of the cells were digitally recorded.

Retroviral vectors

The neomycin selection marker in pLXSN (Clontech) was replaced by a puromycin gene to produce a pLXSP vector bearing the puromycin selection marker. An HA-tagged BCCIPα cDNA was cloned into the *Eco*RI/*Xho*I site of the pLXSP. This vector was used to produce replication deficient virus in a package cell as described (Pear *et al*., 1997). Target cells were infected two times a day for 2 days. Thirty-six hours after the last infection, cells were treated with 1 μg/ml of puromycin for 48 h. The puromycin-resistant cells were changed to fresh medium and incubated for an additional 3 days and counted, or replated for growth curve determinations.

Other procedures

Western blots were performed as described previously (Li *et al*., 2000). Fluorescent *in situ* hybridization (FISH) was performed as described before (Shen *et al*., 1996a) using BCCIP cDNA as the probe. Tumor cell lines were purchased from ATCC.

Abbreviations

GST, glutathion S-transferase; BCCIP, Brca2, Ca and Cip1 interacting protein; DAPI, 4′, 6-diamidino-2-phenylindole; NAD, N-terminus acidic domain; ICD: internal conserved

domain; CVD, C-terminus variable domain; HSF, human skin fibroblast; FISH, fluorescent *in situ* hybridization.

Acknowledgments
We thank Drs Jac Nickoloff and Mark Brenneman for reviewing the manuscript and discussions. This research was supported by NIH NIEHS grant ES08353 and US Army Medical Research and Material Command under DAMD 17-98-1-8198. Its contents are solely the responsibility of the authors and do not necessarily represent the official views of these funding agencies.

References

Bignell G, Micklem G, Stratton MR, Ashworth A and Wooster R. (1997). *Hum. Mol. Genet.*, **6**, 53–58.
Chen CF, Chen PL, Zhong Q, Sharp ZD and Lee WH. (1999). *J. Biol. Chem.*, **274**, 32931–32935.
Gayther SA and Ponder BA. (1998). *Dis. Markers*, **14**, 1–8.
Ittmann M. (1996). *Cancer Res.*, **56**, 2143–2147.
Katagiri T, Saito H, Shinohara A, Ogawa H, Kamada N, Nakamura Y and Miki Y. (1998). *Genes Chrom. Cancer*, **21**, 217–222.
Kim SK, Ro JY, Kemp BL, Lee JS, Kwon TJ, Hong WK and Mao L. (1998). *Oncogene*, **17**, 1749–1753.
Koul A, Nilbert M, Borg A, Cole BF and Arrick BA. (1999). *Genes Chrom. Cancer*, **24**, 207–212.
Li W, Hesabi B, Babbo A, Pacione C, Liu J, Chen DJ, Nickoloff JA and Shen Z. (2000). *Nucleic Acids Res.*, **28**, 1145–1153.
Maier D, Comparone D, Taylor E, Zhang Z, Gratzl O, Van Meir EG, Scott RJ and Merlo A. (1997). *Oncogene*, **15**, 997–1000.
Marmorstein LY, Ouchi T and Aaronson SA. (1998). *Proc. Natl. Acad. Sci. USA*, **95**, 13869–13874.
Milner J, Ponder B, Hughes-Davies L, Seltmann M and Kouzarides T. (1997). *Nature*, **386**, 772–773.
Mollenhauer J, Wiemann S, Scheurlen W, Korn B, Hayashi Y, Wilgenbus KK, von Deimling A and Poustka A. (1997). *Nat. Genet.*, **17**, 32–39.
Nordling M, Karlsson P, Wahlstrom J, Engwall Y, Wallgren A and Martinsson T. (1998). *Cancer Res.*, **58**, 1372–1375.
Pear WS, Scott ML and Nolan GP. (1997). Gene Therapy Protocols. Robbins PD (ed.). Humana Press: Totowa, New Jersey, pp 41–57.
Peiffer SL, Herzog TJ, Tribune DJ, Mutch DG, Gersel, DJ and Goodfellow PJ. (1995). *Cancer Res.*, **55**, 1922–1926.
Petersen S, Rudolf J, Bockmuhl U, Gellert K, Wolf G, Dietel M and Petersen I. (1998). *Oncogene*, **17**, 449–454.
Pontremoli S, Melloni E and Salamino F. (1999). *Calcium as a Cellular Regulator*. Carafoli E and Klee C (eds). Oxford University Press: New York, pp 371–388.
Rasheed BK and Bigner SH. (1991). *Cancer Metastasis Rev.*, **10**, 289–299.
Rasheed BK, McLendon RE, Friedman HS, Friedman AH, Fuchs HE, Bigner DD and Bigner SH. (1995). *Oncogene*, **10**, 2243–2246.
Robertson GP, Herbst RA, Nagane M, Huang HJ and Cavenee WK. (1999). *Cancer Res.*, **59**, 3596–3601.
Sharan SK and Bradley A. (1997). *Genomics*, **40**, 234–241.
Sharan SK, Morimatsu M, Albrecht U, Lim DS, Regel E, Dinh C, Sands A, Eichele G, Hasty P and Bradley A. (1997). *Nature*, **386**, 804–810.
Shen Z, Pardington-Purtymun PE, Comeaux JC, Moyzis RK and Chen DJ. (1996a). *Genomics*, **36**, 271–279.
Shen Z, Peterson SR, Comeaux JC, Zastrow D, Moyzis RK, Bradbury EM and Chen DJ. (1996b). *Mutat Res.*, **364**, 81–89.
Shinohara A, Ogawa H, Matsuda Y, Ushio N, Ikeo K and Ogawa T. (1993). *Nat. Genet.*, **4**, 239–243.
Spain BH, Larson CJ, Shihabuddin LS, Gage FH and Verma IM. (1999). *Proc. Natl. Acad. Sci. USA*, **96**, 13920–13925.
Steck PA, Lin H, Langford LA, Jasser SA, Koul D, Yung WK and Pershouse MA. (1999). *Genes Chrom. Cancer*, **24**, 135–43.
Tan TL, Essers J, Citterio E, Swagemakers SM, de Wit J, Benson FE, Hoeijmakers JH and Kanaar R. (1999). *Curr. Biol.*, **9**, 325–328.
Tanabe S, Akiba T, Katoh M and Satoh T. (1999). *Pediatr. Int.*, **41**, 565–567.
Taysi K, Strauss AW, Yang V, Padmalatha C and Marshall RE. (1982). *Ann. Genet.*, **25**, 141–144.
Vidal M. (1997). *The Yeast Two-Hybrid System*. Bartel PL and Fields S (eds). Oxford University Press: New York, pp 109–147.
Waggoner DJ, Chow CK, Dowton SB and Watson MS. (1999). *Am. J. Med. Genet.*, **86**, 1–5.
Walker GJ, Palmer JM, Walters MK and Hayward NK. (1995). *Genes Chrom. Cancer*, **12**, 134–141.
Wong AKC, Pero R, Ormonde PA, Tavtigian SV and Bartel PL. (1997). *J. Biol. Chem.*, **272**, 31941–31944.
Yano K, Morotomi K, Saito H, Kato M, Matsuo F and Miki Y. (2000). *Biochem. Biophys. Res. Commun.*, **270**, 171–175.
Yjandra N, Bax A, Crivici A and Ikura M. (1999). *Calcium as a Cellular Regulator*. Carafoli, E. Klee, C. (eds). Oxford University Press: New York, pp 152–170.
Yuan SS, Lee SY, Chen G, Song M, Tomlinson GE and Lee EY. (1999). *Cancer Res.*, **59**, 3547–3551.

THE JOURNAL OF BIOLOGICAL CHEMISTRY
© 2001 by The American Society for Biochem

Final report - DAMD17-98-1-8198
Appendix 2

Vol. 276, No. 51, Issue of December 21, pp. 48318–48324, 2001
Printed in U.S.A.

Interaction with BRCA2 Suggests a Role for Filamin-1 (hsFLNa) in DNA Damage Response*

Received for publication, March 21, 2001, and in revised form, September 21, 2001
Published, JBC Papers in Press, October 15, 2001, DOI 10.1074/jbc.M102557200

Yuan Yuan‡§ and Zhiyuan Shen‡¶

From the ‡Department of Molecular Genetics and Microbiology, University of New Mexico School of Medicine, Albuquerque, New Mexico 87131 and the §Graduate Program, Department of Molecular Genetics, School of Medicine, University of Illinois, Chicago, Illinois 60607

The BRCA2 tumor suppressor plays significant roles in DNA damage response. The human actin binding protein filamin-1 (hsFLNa, also known as ABP-280) participates in orthogonal actin network, cellular stress responses, signal transduction, and cell migration. Through a yeast two-hybrid system, an *in vitro* binding assay, and *in vivo* co-immunoprecipitations, we identified an interaction between BRCA2 and hsFLNa. The hsFLNa binding domain of BRCA2 was mapped to an internal conserved region, and the BRCA2-interacting domain of hsFLNa was mapped to its C terminus. Although hsFLNa is known for its cytoplasmic functions in cell migration and signal transduction, some hsFLNa resides in the nucleus, raising the possibility that it participates in DNA damage response through a nuclear interaction with BRCA2. Lack of hsFLNa renders a human melanoma cell line (M2) more sensitive to several genotoxic agents including γ irradiation, bleomycin, and ultraviolet-c light. These results suggest that BRCA2/hsFLNa interaction may serve to connect cytoskeletal signal transduction to DNA damage response pathways.

Inherited *BRCA2* mutations confer profound susceptibility to human breast and ovarian cancers (1, 2). BRCA2 participates in DNA repair through interactions with other proteins, notably RAD51 and BRCA1, that mediate homologous recombination (3–6) but is apparently not required for repair of DNA double-strand breaks by non-homologous end joining (7). The *BRCA2* gene encodes a 3418-amino acid protein with very little homology to other known proteins (1, 2). The overall identity of BRCA2 is 58–59% between rodents (rat and mouse) and human, which is an uncommonly low level of conservation for a tumor suppressor (8, 9). By comparing the amino acid sequences of mouse and human BRCA2, five highly conserved regions have been identified within BRCA2 and designated as Domain I through Domain V (8). It is expected that important functions of BRCA2 reside in these conserved regions.

Domain I resides in amino acids (aa)[1] 1–100 and is a putative transcriptional activation domain (10). Domain II (aa 1001–1051 of human, aa 980–1030 of mouse) and Domain III (aa 1089–1138 of human, aa 1072–1120 of mouse) reside in exon 11 (8), which also contains the eight loosely conserved BRC motifs (11) that mediate interaction with RAD51 (12, 13). The first BRC motif overlaps Domain II. Domain IV (aa 2479–3157 of human; aa 2400–3075 of mouse) is coded by exons 14–24 (8). Domain V (aa 3267–3316 of human; aa 3190–3238 of mouse) is encoded by exon 27 and also mediates BRCA2/RAD51 interaction (14). A putative nuclear localization signal also resides in exon 27 (15).

Domain IV is the longest of the conserved domains, yet the least understood. In mouse, two mutations delete some of the BRC repeats (truncation at aa 1492 deleting BRC repeat 4–8 and truncation at aa 2014 deleting BRC repeat 8), together with conserved Domains IV and V. Both result in partial lethality of embryos and infertility, as well as enhanced expression of p21 and p53 (4, 16–18). However, truncation of mouse BRCA2 at aa 3140, which preserves all of the BRC repeats plus Domain IV and deletes only Domain V, results in no p21 and p53 induction (19). Mice with this truncation have much higher rate of viability and are fertile.[2] The difference in phenotype between truncation at aa 2014 and truncation at aa 3140 indicates that important functions might reside in Domain IV and its flanking BRC8 repeat.

Recently, a few protein interaction partners of Domain IV have been identified. A protein named DSS1 (Deleted in Split hand/Split foot) interacts with aa 2472–2957 within Domain IV (20). The function of human DSS1 is uncertain. The yeast DSS1 homologue (also termed SEM) plays roles in cell growth and differentiation (21). A second protein named hBUBR1 interacts with aa 2867–3176 of Domain IV and affects the phosphorylation status of BRCA2 (22). hBUBR1 and its yeast homologues contain a kinase domain, and may participate in mitotic checkpoint control (22–24). We have also identified a novel protein, designated BCCIPα (Brca2, and cip1 interacting protein) that interacts with Domain IV (25). BCCIPα is an evolutionarily conserved protein that may participate in the regulation of tumorigenesis (25).

Here, we report an interaction of the BRCA2-conserved Domain IV with the actin-binding protein hsFLNa (human nonmuscle filamin-1). hsFLNa (also known as ABP-280) is an actin cross-linking protein (26) that participates in cytoskeletal remodeling, signal transduction, and protein nuclear translocation (for a review see Ref. 27). hsFLNa interacts with several partners, including β_1 and β_2 integrins, Rho GTPase, SEK-1, and human androgen receptor (28–33). In addition, we report that hsFLNa-deficiency in human cells is associated with cel-

* This research was supported by NIEHS National Institutes of Health Grant ES08353 and by the United States Army Medical Research and Materiel Command under DAMD17-98-1-8198. The costs of publication of this article were defrayed in part by the payment of page charges. This article must therefore be hereby marked "*advertisement*" in accordance with 18 U.S.C. Section 1734 solely to indicate this fact.

¶ To whom correspondence should be addressed: Dept. of Molecular Genetics and Microbiology, Univ. of New Mexico School of Medicine, 915 Camino de Salud, NE, Albuquerque, NM 87131, Tel.: 505-272-4291; Fax: 505-272-6029; E-mail: zshen@salud.unm.edu.

[1] The abbreviations used are: aa, amino acids; UV-C, ultraviolet-c; GST, glutathione-*S*-transferase; Co-IP, co-immunoprecipitation; HA, hemagglutinin; PBS, phosphate-buffered saline; DAPI, 4′,6-diamidino-2-phenylindole; MAPK, mitogen-activated protein kinase.

[2] P. Hasty, personal communication.

lular sensitization to DNA-damage agents such as γ irradiation, bleomycin, and UV-C. These data suggest a functional affiliation of hsFLNa with the DNA damage response pathway.

MATERIALS AND METHODS

Yeast Two-hybrid System—The yeast Matchmaker two-hybrid system (CLONTECH Laboratory, Palo Alto, CA) was used for a library screen as described in a previous publication (25). In brief, BRCA2H (aa 2883–3053), a BRCA2 fragment, was cloned into the Gal4-DNA binding domain (Gal4-DB) vector (pAS2–1) to screen a library of human lymphocyte cDNAs fused to the Gal4-DNA activation domain (Gal4-DA) vector (pACT). MV103 cells were used as the host strain (34). An independent yeast host strain (SFY526) and vectors (pGBT9 and pGAD424) were used to confirm the interaction identified in the library screen. Yeast two-hybrid filter assays and liquid quantitative assays were performed according to the Matchmaker manual. pGBT9 and pGAD424 were used as negative controls.

Recombinant Proteins—To express a His-tagged hsFLNa fusion protein, an hsFLNa C-terminal fragment (aa 2250–2647) was cloned into pET28a (Novagen) and transformed into *Escherichia coli* BL21 (DE3). His/hsFLNa fusion protein expression and purification was performed as described previously (25, 35, 36). To fuse glutathione *S*-transferase (GST) with fragments of BRCA2, various coding regions of BRCA2 were amplified by PCR and cloned into pGEX-5X-1 or pGEX-5X-3. These plasmids were transformed into competent *E. coli* BL21, and the expression and purification of GST fusion proteins were performed as previously described (25, 35, 36).

In Vitro Protein Binding Assay—GST or GST/BRCA2 fragments bound to glutathione-Sepharose beads were incubated with 10 μg of purified His/hsFLNa (aa 2250–2647) in binding buffer (100 mM KCl, 50 mM Tris, pH 7.9, 12.5 mM $MgCl_2$, 1 mM EDTA, 10% glycerol) for 1 h at 4 °C. Beads were washed three times with wash buffer I (100 mM NaCl, 50 mM Tris, pH 7.9, 1 mM EDTA, 0.1% Nonidet P-40) and three times with wash buffer II (200 mM NaCl, 50 mM Tris, pH 7.9, 1 mM EDTA, 0.1% Nonidet P-40). The beads were collected and resuspended in 2× sample buffer. Samples were boiled for 5 min and separated by SDS-PAGE. Proteins were then transferred to polyvinylidene difluoride membrane, and co-precipitated His/hsFLNa proteins were detected by immunoblotting with anti-His antibody and anti-GST antibody (Santa Cruz). Proteinase inhibitor mixture (Sigma) was used in the lysis, binding, and washing buffers.

Co-immunoprecipitation (Co-IP)—Two BRCA2 fragments, BRCA2F (aa 2883–3418) and BRCA2B (aa 2883–3194), were cloned into pHA-CMV vector to tag them with the HA epitope. The C terminus of hsFLNa (aa 2250–2647) was cloned into pMyc-CMV vector to tag it with the Myc epitope. Plasmids were transfected into 293 human kidney cells using GenePorter transfection reagent (GeneTherapy Systems). Forty-eight hours after transfection, cells were collected, treated with lysis buffer (150 mM NaCl, 1 mM EDTA, 50 mM Tris-HCl, pH 7.5, 1% Nonidet P-40, 1× protease inhibitors (Boehringer)), sonicated, and centrifuged for 10 min at 10,000 rpm. The supernatant (whole cell lysate) was used for immunoprecipitation. Forty microliters of anti-HA affinity matrix (Roche Molecular Biochemicals) was incubated with 1 mg of whole cell lysate at 4 °C on a rocker for 20 min. The matrix was then washed six times in wash buffer (200 mM NaCl, 1 mM EDTA, 50 mM Tris-HCl, pH 7.5, 1% Nonidet P-40, 1× protease inhibitors). Proteins retained on the beads were eluted with 2× SDS sample buffer by boiling for 5 min. Western blotting was performed using anti-HA polyclonal antibody (CLONTECH) and anti-Myc monoclonal antibody (CLONTECH).

To precipitate endogenous BRCA2, cells were lysed in lysis buffer (50 mM HEPES, pH 7.6, 250 mM NaCl, 5 mM EDTA, 0.1% Nonidet P-40). Two milligrams of protein were incubated with 4 μg of BRCA2 antibody (Ab-1, Oncogene) for 1.5 h, protein A plus G beads (Santa Cruz) were added for an additional 2 h. Beads were collected and washed ten times in lysis buffer. Then 2× SDS sample buffer was added and heated at 55 °C for 10 min. Samples were resolved by 5% PAGE gel.

Immunostaining and Confocal Microscopy of hsFLNa—Cells were cultured in chamber slides (Nalge Nunc International) for 12 h, fixed with PBS-buffered paraformaldehyde solution (3% paraformaldehyde, PBS, pH 7.4, 2% sucrose) for 30 min and permeabilized in permeabilization solution (0.5% Triton X-100, 20 mM HEPES, pH 7.4, 50 mM NaCl, 3 mM $MgCl_2$, 300 mM sucrose) for 15 min. Slides were blocked by a 30-min incubation with 2% bovine serum albumin in PBS and then incubated with primary antibody (monoclonal anti-filamin antibody, Chemicon) at 4 °C overnight. Nonspecific mouse IgG was used as a negative control. The cells were incubated with fluorescein isothiocyanate-conjugated anti-mouse IgG secondary antibody (Pierce) for 30 min. The stained cells were mounted under coverslips with Vectashield mounting medium containing DAPI (Vector Laboratories). Immunofluorescence was recorded using the Zeiss confocal microscope LSD 510 with Ar/Kr and UV laser sources.

Cellular Protein Fractionation—To prepare whole cell protein extracts, HeLa cells were trypsinized, washed in ice-cold PBS, pelleted, resuspended in lysis buffer (50 mM HEPES/KOH, pH 7.5, 250 mM NaCl, 1 mM EDTA, 2.5 mM EGTA, 0.1% Tween 20, 10% glycerol, 10 mM β-glycerophosphate, 1 mM dithiothreitol, 1 mM NaF, 0.1 mM Na_3VO_5, 0.2 mM phenylmethylsulfonyl fluoride, 20 μg/ml aprotinin, 20 μg/ml leupeptin) and sonicated for 30 s. Insoluble debris was removed from extracts by centrifugation at 14,000 rpm for 8 min, and the soluble fractions were retained as whole cell extracts. To prepare nuclear and cytoplasmic extracts, HeLa cells were trypsinized, washed in PBS and then in buffer X (25 mM Tris-HCl, pH 7.5, 50 mM NaCl, 5 mM EDTA, 1× protease inhibitors (Boehringer)), pelleted, and resuspended in buffer X containing 0.5% Nonidet P-40 for 10 min on ice. The lysate was centrifuged at 15,000 rpm for 5 min at 4 °C. The supernatant was taken as the cytoplasm/membrane fraction. The remaining nuclear pellet was washed with buffer X containing 0.5% Nonidet P-40 and resuspended in the same buffer containing 1× loading buffer. The samples were then sonicated and boiled before loading onto the SDS-PAGE gel.

Cell Culture—Human M2 and A7 cells were kindly provided by Drs. T. P. Stossel and Y. Ohta (Brigham and Women's Hospital, Harvard Medical School). M2 is a human melanoma cell line lacking hsFLNa expression. The A7 cell line was derived from M2 by stably transfecting with a plasmid expressing full-length hsFLNa cDNA (37). Cells were subcultured twice a week in minimum essential medium Eagle with Earle's salt (EMEM) (M2) or EMEM with 0.5 mg/ml G418 (A7). MCF-7 cells and Capan-1 cells were obtained from ATCC and cultured as recommended. All media contained 10% fetal bovine serum and 1% penicillin/streptomycin.

Genotoxin Sensitivity Assays—The number of cells to be plated for each assay was determined by a pilot experiment so as to yield 50–100 surviving colonies per 100-mm plate. For radiation sensitivity assay, 18 h after the cells were plated cells were irradiated with a Cs-137 γ rays (dose rate: 1.05 Gray/min). For UV-C sensitivity assay, the UV-C exposure was achieved at 1.3 $J/m^2/s$ dose rate. For bleomycin sensitivity assay, exponentially growing cells were treated with bleomycin for 2 h, trypsinized, and plated. In all the assays, cells were incubated for 12–14 days for colony formation. The colonies were stained with crystal violet and counted to determine cell viability. The number of colonies was normalized to the number of cells plated to calculate the surviving fraction.

RESULTS AND DISCUSSION

A C-terminal Domain of hsFLNa Interacts with BRCA2 in a Yeast Two-hybrid System—A portion of BRCA2 Domain IV comprising amino acids 2883–3053 (designated BRCA2H) was used as "bait" for a yeast two-hybrid screen. BRCA2H is 77% identical between human and mouse, compared with the overall identity of 58–59% (8). Nine independent clones containing the C terminus of hsFLNa were isolated from a total of 4×10^5 independent clones. The interaction of these nine clones with BRCA2H was confirmed using a second, independent yeast two-hybrid system (SFY526 instead of MV103 as host yeast, pGBT9 instead of pAS2–1 and pGAD424 instead of pACT as vectors).

To further map the region of hsFLNa required for interaction with BRCA2H, defined C-terminal portions of hsFLNa were tested in the yeast two-hybrid system. hsFLNa is an elongated homodimeric, Y-shaped structure (26). Each monomer consists of an N-terminal actin binding domain followed by 24 tandem repeats, each ~96 amino acids in length. The last 65 amino acids of its C terminus contain a self-assembly sequence that allows dimerization. This repeat is separated from the previous 23 repeats by an ~34-amino acid "hinge" domain. Ten hsFLNa constructs containing tandem repeats and/or the hinge region, as described in Fig. 1, were cloned into pGAD424. Each of the ten constructs was co-expressed with Gal4-DB/BRCA2H fusion protein in SFY526 cells and tested for interaction. The largest construct tested, comprising aa 2250–2647, represents the

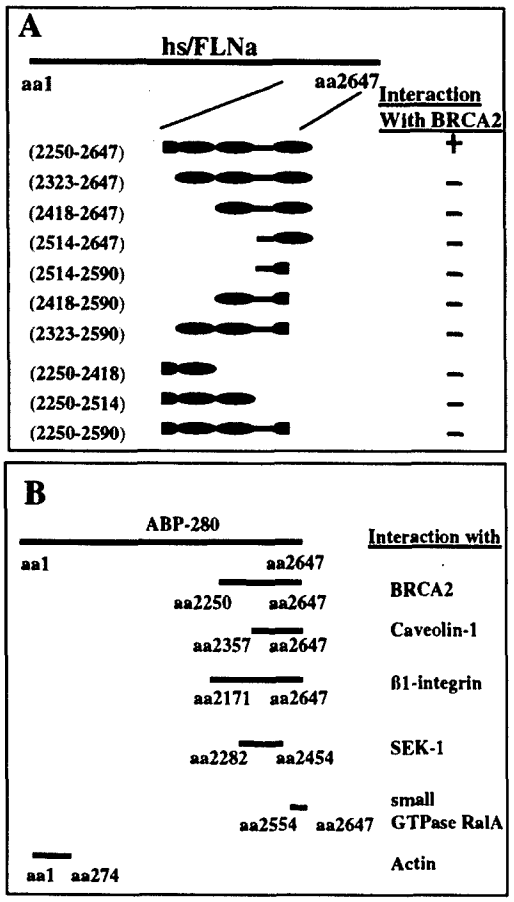

FIG. 1. **Mapping of the BRCA2-interacting domain in hsFLNa by a yeast two-hybrid system.** *A*, ten regions of hsFLNa were fused with Gal4-DA and tested for interaction with Gal4-DB-fused BRCA2H. "+" indicates a positive interaction, and "–" indicates no detectable interaction in the two-hybrid system. The *filled black ovals* represent tandem repeats 21–24; the *line* between tandem repeat 23 and 24 represents the hinge region. The constructs were prepared according to the boundaries of the tandem repeats and the hinge region. The first construct contains the last ~3.5 repeats. The next three constructs encode hsFLNa fragments progressively lacking tandem repeats from the N terminus. The following three contain the same sequence as the above three except lacking the C-terminal self-interaction domain. The last three encode hsFLNa fragments progressively lacking the self-interaction domain and the tandem repeats from the C terminus. *B*, a summary of several interacting proteins for hsFLNa.

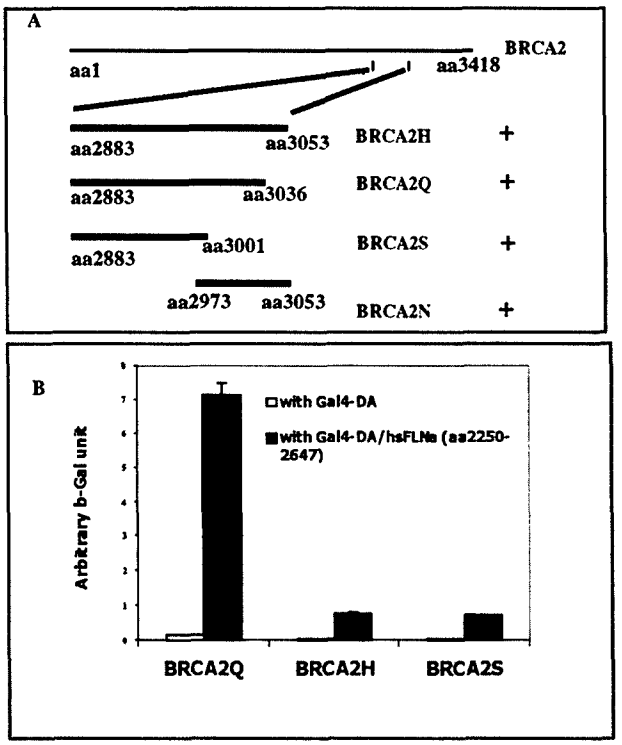

FIG. 2. **Mapping of the hsFLNa-interacting domain in BRCA2 by a yeast two-hybrid system.** *A*, four fragments of BRCA2 Domain IV were fused to Gal4-DB to produce Gal4-DB/BRCA2H, Gal4DB/BRCA2Q, Gal4-DB/BRCA2S, and Gal4-DB/BRCA2N and tested for interaction with Gal4-DA/hsFLNa (aa 2250–2647); "+" indicates a positive interaction. *B*, quantitative LacZ assay of the constructs BRCA2H, BRCA2Q, and BRCA2S in *A*.

minimum region of hsFLNa required for interaction with BRCA2. This region is also known to interact with several other proteins (Fig. 1*B*) (Please see Ref. 27 and citations therein).

Mapping of the hsFLNa-interacting Domain in BRCA2—To map the hsFLNa binding domain in BRCA2, four BRCA2 fragments were constructed: BRCA2H (aa 2883–3053), BRCA2Q (aa 2883–3036), BRCA2S (aa 2883–3001), and BRCA2N (aa 2973–3053) (Fig. 2*A*). These constructs were tested for interaction with hsFLNa (aa 2250–2647) in a filter assay (Fig. 2*A*). BRCA2H, BRCA2Q, and BRCA2S were also tested in a quantitative yeast two-hybrid assay (Fig. 2*B*). Based on these data, the putative hsFLNa binding site can be assigned to a small region common to these constructs, namely aa 2973–3001 of BRCA2.

Although the yeast two-hybrid assays demonstrate that hsFLNa and BRCA2 interact, it was not clear whether this interaction is a direct BRCA2/hsFLNa binding or mediated by other protein(s) in yeast. To further test whether hsFLNa directly binds to BRCA2, an *in vitro* protein-binding assay using purified recombinant proteins was performed. The BRCA2-interacting domain of hsFLNa (aa 2250–2647) was fused with a His_6 tag. Various regions of BRCA2 were fused with GST and summarized in Fig. 3*C*. The BRCA2/GST fusion proteins were purified to near-homogeneity and used to precipitate His/hsFLNa (aa 2250–2647) fusion protein (Fig. 3, *A* and *B*). None of the negative controls bound to His/hsFLNa (aa 2250–2647) (Fig. 3, *A* and *B*, *lanes 2*, *3*). GST/BRCA2S (aa 2883–3001) and GST/BRCA2N (aa 2973–3053) co-precipitate His/hsFLNa (aa 2250–2647). Since aa 2973–3001 is the region shared by BRCA2N and BRCA2S, we conclude that BRCA2 (aa 2973–3001) is the minimal domain for interaction with hsFLNa, consistent with the yeast two-hybrid data.

We noticed that BRCA2Q (aa 2883–3036) interacts with hsFLNa in the yeast two-hybrid system but fails to bind hsFLNa *in vitro* and that BRCA2P (aa 2973–3041) contains aa 2973–3001 but fails to bind hsFLNa *in vitro* (Fig. 3*C*). This inconsistency may be caused by the different protein contexts of Gal4 *versus* GST fusions or the folding of the recombinant GST/BRCA2Q and GST/BRCA2P proteins such that the interaction domain is covered.

BRCA2 Interacts with hsFLNa in Vivo—To confirm that complex formation between BRCA2 and hsFLNa occurs *in vivo*, Co-IP was performed in mammalian cells. Both exogenously expressed and endogenous proteins were tested. Because smaller fragments of BRCA2 (BRCA2H, BRCA2Q, BRCA2S, and BRCA2N) exhibited limited solubility when tagged with an HA epitope (data not shown), longer BRCA2 constructs, BRCA2B (aa 2883–3194) and BRCA2F (aa 2883–3418), were used for exogenously expressed proteins. Both of the latter contain the minimal hsFLNa-interacting domain of BRCA2, aa 2973–3001. A C-terminal hsFLNa fragment (aa 2250–2647) was tagged with a Myc epitope. Myc/hsFLNa (aa 2250–2647) was co-expressed in 293 human kidney cells with HA/BRCA2B

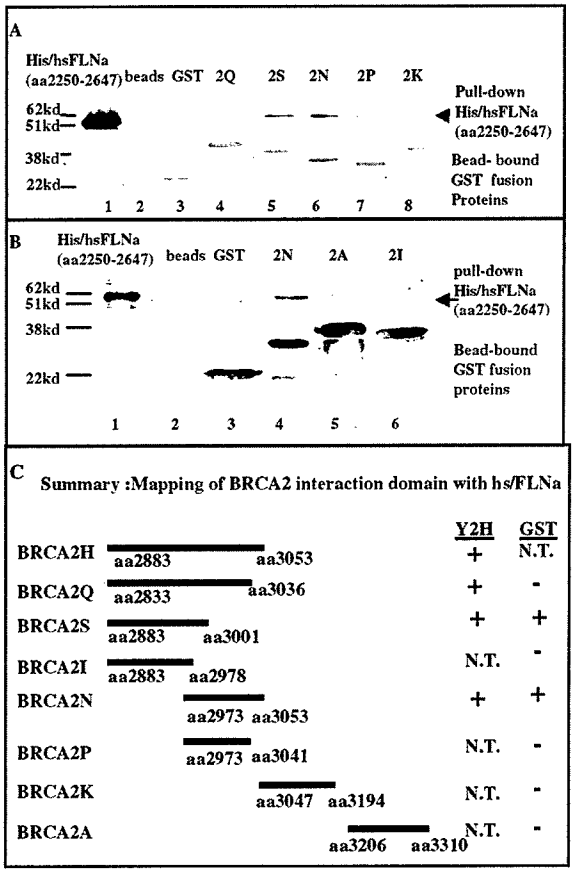

FIG. 3. **Mapping of the hsFLNa-interacting domain in BRCA2 by *in vitro* binding assay.** *A* and *B*, equal amounts of bead-bound GST/BRCA2 fusion proteins (*bottom panel*) were incubated with 10 μg of purified hsFLNa at 4 °C for 1 h and washed, and the retained proteins were subjected to SDS-PAGE and immunoblotted with anti-His (*top panel*) or anti-GST antibody (*bottom panel*). The GST-fusion BRCA2 fragments used in the assay are labeled on the top of the panel. *Lane 1* is purified His/hsFLNa (aa 2250–2647) alone as a positive control. *Lane 2* and *lane 3* are the binding of His/hsFLNa (aa 2250–2647) with the resin or GST protein as negative controls. Result from *lanes 2* and *3* suggest that the His/hsFLNa protein does not bind to the resin alone or to the GST protein alone. *C*, comparison of the hsFLNa binding domain mapped by the yeast two-hybrid system (Fig. 2*A*) and *in vitro* binding system (Fig. 3, *A*, *B*). *N.T.*, Not Tested. +, positive interaction. −, no interaction.

or HA/BRCA2F, or with empty HA vector or a non-relevant protein, HA/BCCIPα (25), as negative controls. The HA-tagged proteins were immunoprecipitated with anti-HA affinity matrix, and co-precipitated Myc/hsFLNa (aa 2250–2647) was detected by anti-Myc antibody. As shown in Fig. 4 (*top panel*), HA/BCCIPα (*lane 6*) or HA vector (*lane 9*) did not co-precipitate Myc/hsFLNa (aa 2250–2647). On the other hand, HA/BRCA2B (*lane 7*) and HA/BRCA2F (*lane 8*) co-precipitate Myc/hsFLNa (aa 2250–2647). These data suggest a stable complex between BRCA2 and hsFLNa *in vivo*.

To investigate the endogenous protein complex, MCF-7 and Capan-1 cells were used. MCF-7 expresses the wild type BRCA2 protein, while Capan-1 cell contains the 6174delT mutation that produces an ~230-kDa C-terminally truncated protein lacking the hsFLNa interaction domain. We used an anti-BRCA2 antibody (Ab-1, Oncogene) that reacts with both the full-length and the 230-kDa-truncated BRCA2 protein for immunoprecipitation. The immunoprecipitated BRCA2 protein complex was immunoblotted with anti-hsFLNa and anti-BRCA2. As shown in Fig. 4*B*, both the wild type BRCA2 from MCF-7 cells and the truncated BRCA2 from Capan-1 cells were precipitated with the anti-BRCA2 antibody (*lanes 3* and *4* of *bottom panel*). Both MCF-7 and Capan-1 cells express hsFLNa protein (*lanes 1* and *2* of *top panel*). However, only the endogenous hsFLNa from MCF-7 was co-precipitated with BRCA2 (*lane 3*, *top panel*), but not from Capan-1 cells (*lane 4*, *top panel*). These further indicate that a stable complex exists *in vivo* between full-length BRCA2 and hsFLNa and that the C-terminal region deleted in Capan-1 cells is required for the interaction.

A Fraction of hsFLNa Resides in the Nucleus—BRCA2 has been described as a predominant nuclear protein (39). hsFLNa is thought to execute most of its functions in the cytoplasm (26, 27, 29–33, 40–42), although it may participate in nuclear-related functions (28). It might be argued that the interaction between hsFLNa and BRCA2 is not physiologically relevant since they apparently reside in different cellular compartments. To address this issue, we performed immunostaining of hsFLNa in human skin fibroblast and HeLa cells to observe the distribution of hsFLNa with confocal microscopy, which detects fluorescent signals from a thin intersection of 0.5 μm within the cells. The majority of hsFLNa was seen in the cytoplasmic compartment of the cells (Fig. 5, *B*, *C*, *E*, *F*), which is consistent with previous reports (26, 27, 29–33, 40–42). However, a moderate level of hsFLNa signal was seen in the nucleus as well, suggesting that a fraction of hsFLNa resides in the nucleus. To further demonstrate that hsFLNa exists in the nucleus, the cytoplasmic and nuclear proteins were extracted from HeLa cells and analyzed by Western blot. As shown in Fig. 5*G*, hsFLNa protein was detected in both the cytoplasmic and nuclear fractions. YY1 and paxillin are used as nuclear and cytoplasmic controls, respectively.

Lack of hsFLNa Does Not Affect Cell Growth but Renders Cells More Sensitive to Genotoxic Agents—The diverse interaction partners of hsFLNa suggest its multiple functions in different cellular processes (27). Characterization of these interacting proteins has provided major insights into the roles of hsFLNa. For instance, hsFLNa was related to integrin signaling pathways through its association with β_1, β_2, and β_7 integrins (31, 32, 43, 44). The physiological significance of hsFLNa was suggested by the discovery of an X-linked dominant human disorder, periventricular heterotopia, caused by mutations in the *hsFLNa* gene. Mutations are embryonic lethal in males; in females, they are characterized by defects in the migration of cerebral cortical neurons and vascular abnormalities (45, 46). These results are consistent with the previous observation that hsFLNa is essential for melanocyte migration *in vitro* (37), suggesting that hsFLNa might be a key protein in cell migration. Similarly, hsFLNa was connected to the MAPK cascade through its associations with SEK-1 and TRAF2 (tumor necrosis factor receptor-associated factor 2) (33, 47). Taking the above examples together, the association of hsFLNa with BRCA2 suggests its involvement in BRCA2-mediated DNA damage response.

BRCA2 plays important roles in DNA damage response, possibly by participating in homologous recombinational repair and/or by mediating signal transduction that affects other cellular responses to DNA damage. To evaluate whether hsFLNa is also involved in DNA damage response, we used the hsFLNa-deficient human M2 melanoma cell line and an isogenic hsFLNa-proficient derivative line, A7. M2 (hsFLNa$^-$) cells have impaired locomotion and display circumferential blebbing of the plasma membrane. The hsFLNa expression has been restored to approximately normal level in A7 cells by stable transfection with an hsFLNa expression vector. A7 cells have restored translocational motility and reduced membrane blebbing (37, 42). As confirmed in Fig. 6*A*, A7 cells express hsFLNa, but M2 cells do not. Lack of hsFLNa does not affect the growth

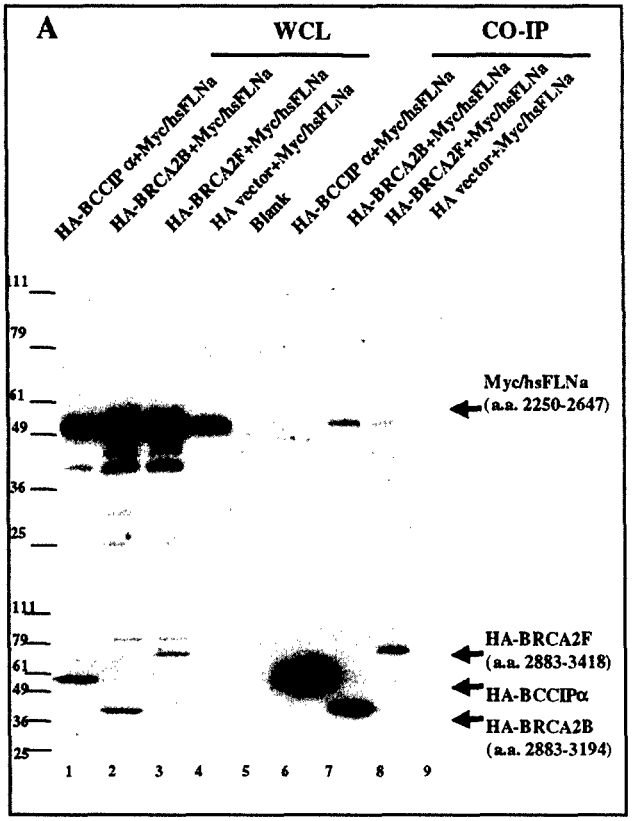

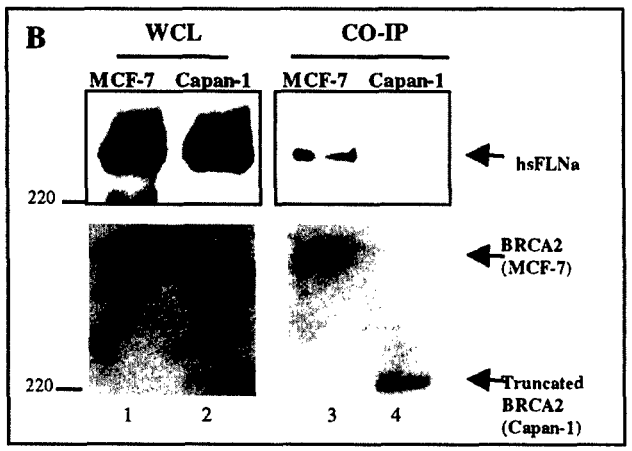

FIG. 4. ***In vivo* interactions of BRCA2 and hsFLNa.** *A*, Myc/hsFLNa (aa 2250–2647) interacts with HA/BRCA2B (aa 2883–3194) or HA/BRCA2F (aa 2883–3418). HA/BCCIPα, HA/BRCA2B (aa 2883–3194), HA/BRCA2F (aa 2883–3418), or empty HA vector was co-expressed with Myc/hsFLNa (aa 2250–2647) in 293 human kidney cells. The HA-tagged proteins were immunoprecipitated with anti-HA affinity matrix. Co-immunoprecipitated Myc/hsFLNa (aa 2250–2647) was detected by anti-Myc antibody (*top panel*), and HA-tagged proteins were detected with anti-HA antibody (*bottom panel*). *Lanes 1–4* show the protein from whole cell lysate (*WCL*), and *lanes 6–9* are the precipitated proteins. *Lane 5* is a blank. Myc/hsFLNa co-precipitates with HA-BRCA2B (aa 2883–3194) (*lane 7*) and HA-BRCA2F (aa 2883–3418) (*lane 8*), but not HA-BCCIPα (*lane 6*) or the HA vector control (*lane 9*). *B*, endogenous BRCA2 interacts with hsFLNa. Whole cell lysate (*WCL*) from MCF-7 and Capan-1 cells were incubated with anti-BRCA2 (Ab1, Oncogene) that reacts with amino acids 1651–1821 of BRCA2 in both MCF-7 and Capan-1 cells. The precipitated BRCA2 complex was immunoblotted with anti-hsFLNa antibody (*top panel*) and anti-BRCA2 antibody (*bottom panel*). In the *bottom panel*, full-length BRCA2 from MCF-7 (*lane 1*) or truncated BRCA2 from Capan-1 (*lane 2*) is detected in whole cell lysate as well as the immunoprecipitated complex (*lanes 3* and *4*). However, hsFLNa is only co-precipitated with the full-length BRCA2 in MCF-7 cells (*lane 3, top panel*) but not with the truncated BRCA2 in Capan-1 cells (*lane 4, top panel*). This figure shows that the endogenous full-length BRCA2 in MCF-7 co-precipitates the endogenous hsFLNa protein. However, the C-terminally deleted BRCA2 in Capan-1 cells could not co-precipitate endogenous hsFLNa protein. It not only demonstrates that the endogenous BRCA2 and hsFLNa interact but also demonstrates that the C-terminal region deleted in Capan-1 cells is required for the hsFLNa/BRCA2 interaction.

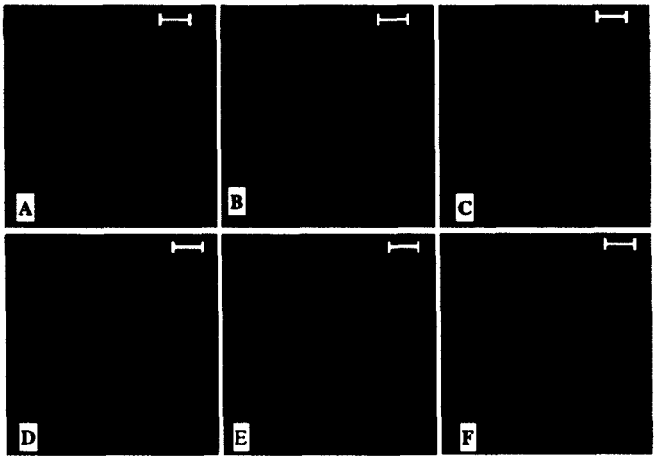

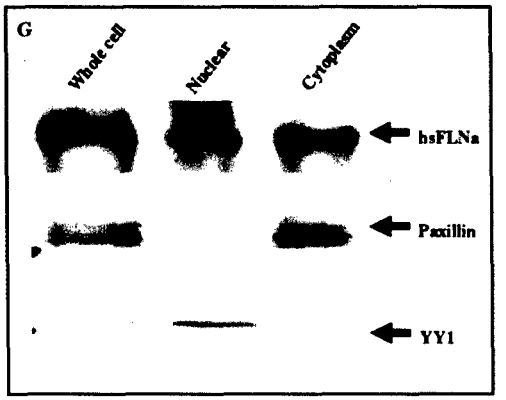

FIG. 5. **Nuclear and cytoplasmic distribution of hsFLNa in human skin fibroblast (*A–C*) and HeLa (*D–F*) cells.** *A* and *D*, the nucleus was visualized by DAPI staining (*blue*). *B* and *E*, hsFLNa was visualized as *green*. *C* and *F*, superimposed illustration for both the nuclear signals and hsFLNa signals. *Bar*, 20 μm. *G*, Western blot of hsFLNa distribution in cytoplasmic and nuclear fractions of HeLa cells. The whole cell lysate, nuclear, and cytoplasmic fractions of HeLa cells were separated by SDS-PAGE gel and blotted with hsFLNa antibody (*top panel*). The same membrane was re-blotted with anti-paxillin (cytoplasmic protein) antibodies (*middle panel*) and anti-YY1 (nuclear protein) antibodies (*bottom panel*) as positive controls for nuclear and cytoplasmic fraction, respectively. About three times more of nuclear extracts were loaded for Western analysis, as evidenced by the YY1 level.

of M2 cells in culture (Fig. 6*B*). A7 ($hsFLNa^+$) and M2 ($hsFLNa^-$) cells have similar plating efficiencies (50–70%). However, when treated with γ radiation, bleomycin, and UV-C light, M2 cells ($hsFLNa^-$) were markedly more sensitive than A7 cells ($hsFLNa^+$), as assessed in colony formation assays (Fig. 6, *C–E*).

DNA double-strand break is the major damage caused by ionizing radiation, which is repaired by a variety of pathways including recombinational repair. Bleomycin is believed to generate oxygen radicals that damage DNA in a similar manner to ionizing radiation. Whereas pyrimidine dimer is the major damage caused by UV-C light, which is predominantly repaired by nucleotide excision repair. As the results shown, deletion of hsFLNa causes increased sensitivity to several distinct genotoxic agents, establishing that hsFLNa plays an essential role for cells to survive DNA damage.

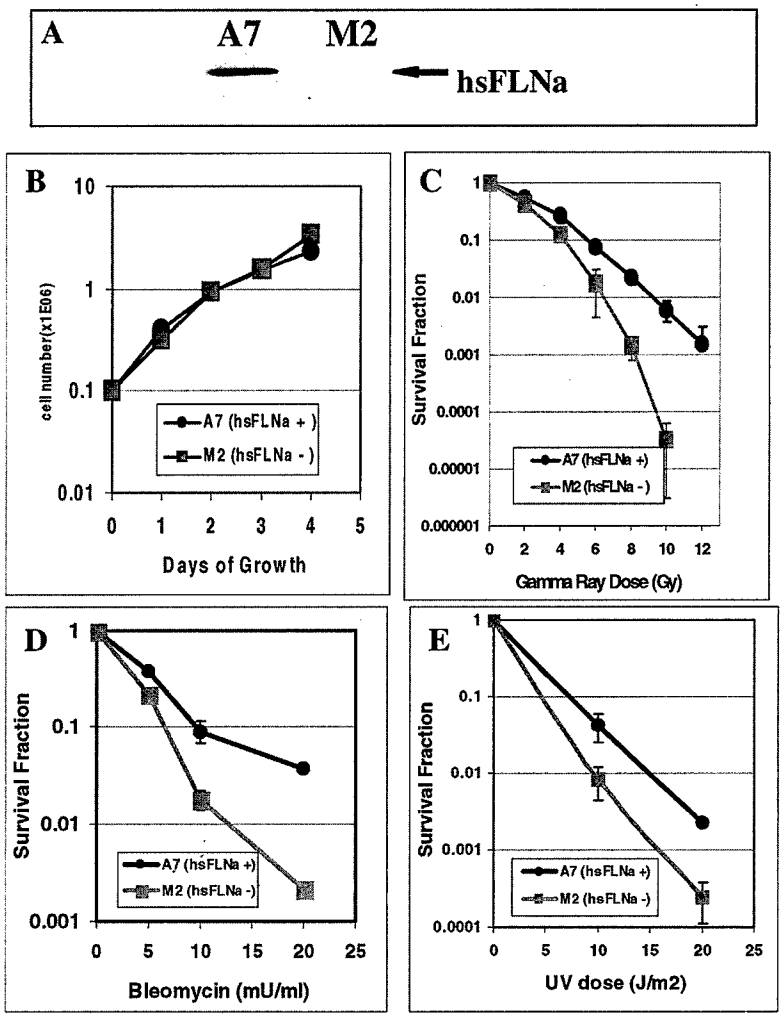

FIG. 6. **Lack of hsFLNa does not affect cell growth but renders melanoma cells more sensitive to genotoxic agents.** *A*, hsFLNa level in A7 and M2 cells. M2 lacks hsFLNa expression. *B*, the growth rates of M2 and A7 cells *in vitro* (data are average of three growth curves). M2 and A7 cells have similar plating efficiency as determined by colony formation assay (data not shown). *C*, *D*, and *E*, survival fractions of A7 and M2 cells to γ irradiation (*C*), bleomycin (*D*), and UV-C (*E*). Survival fractions were measured by clonogenic assay. Shown are averages of three to five independent experiments. *Error bars* indicate standard errors of the averages.

In summary, we have demonstrated an interaction between BRCA2 and hsFLNa by yeast two-hybrid analyses, an *in vitro* binding assay, and *in vivo* Co-IP. The interaction domains of BRCA2 and hsFLNa for this interaction have been mapped. The identified hsFLNa binding domain of BRCA2 resides in the conserved Domain IV of BRCA2 encoded by exons 14–24. This longest-conserved region of BRCA2 interacts with several other proteins as well, including DSS1 (20), BCCIPα (25), and hBUBR1 (22). These proteins are involved in a variety of cell functions, such as growth control, cell cycle regulation, and signal transduction. Therefore, Domain IV may be a particularly important region for the functions of BRCA2 in tumorigenesis. We have also found that deficiency of hsFLNa renders cells more sensitive to γ radiation, bleomycin, and UV-C light. The results suggest that the interaction between hsFLNa and BRCA2 may represent an important link between BRCA2-mediated DNA damage response and cytoskeletal signal transduction pathways.

Acknowledgments—We thank Drs. T. P. Stossel and Y. Ohta (Brigham and Women's Hospital, Harvard Medical School) for generously providing the M2 and A7 melanoma cell lines, Jun Huan for an initial yeast two-hybrid analysis, Jingmei Liu for providing the BRCA2B and BRCA2F fragments, and Dr. Mark Brenneman for reviewing the manuscript.

REFERENCES

1. Wooster, R., Bignell, G., Lancaster, J., Swift, S., Seal, S., Mangion, J., Collins, N., Gregory, S., Gumbs, C., Micklem, G., *et al.* (1995) *Nature* **378,** 789–792
2. Couch, F. J., Farid, L. M., DeShano, M. L., Tavtigian, S. V., Calzone, K., Campeau, L., Peng, Y., Bogden, B., Chen, Q., Neuhausen, S., Shattuck-Eidens, D., Godwin, A. K., Daly, M., Radford, D. M., Sedlacek, S., Rommens, J., Simard, J., Garber, J., Merajver, S., and Weber, B. L. (1996) *Nat. Genet.* **13,** 123–125
3. Chen, J. J., Silver, D., Cantor, S., Livingston, D. M., and Scully, R. (1999) *Cancer Res.* **59,** (suppl.) 1752–1756
4. Patel, K. J., Yu, V. P., Lee, H., Corcoran, A., Thistlethwaite, F. C., Evans, M. J., Colledge, W. H., Friedman, L. S., Ponder, B. A., and Venkitaraman, A. R. (1998) *Mol. Cell* **1,** 347–357
5. Venkitaraman, A. R. (1999) *Science* **286,** 1100–1102
6. Marmorstein, L. Y., Ouchi, T., and Aaronson, S. A. (1998) *Proc. Natl. Acad. Sci. U. S. A.* **95,** 13869–13874
7. Wang, H., Zeng, Z., Bui, T., DiBiase, S., Qin, W., Xia, F., Powell, S., and Iliakis, G. (2001) *Cancer Res.* **61,** 270–277
8. Sharan, S. K., and Bradley, A. (1997) *Genomics* **40,** 234–241
9. McAllister, K. A., Haugen-Strano, A., Hagevik, S., Brownlee, H. A., Collins, N. K., Futreal, P. A., Bennett, L. M., and Wiseman, R. W. (1997) *Cancer Res.* **57,** 3121–3125
10. Milner, J., Ponder, B., Hughes-Davies, L., Seltmann, M., and Kouzarides, T. (1997) *Nature* **386,** 772–773
11. Bignell, G., Micklem, G., Stratton, M. R., Ashworth, A., and Wooster, R. (1997) *Hum. Mol. Genet.* **6,** 53–58
12. Chen, P. L., Chen, C. F., Chen, Y., Xiao, J., Sharp, Z. D., and Lee, W. H. (1998) *Proc. Natl. Acad. Sci. U. S. A.* **95,** 5287–5292
13. Wong, A. K. C., Pero, R., Ormonde, P. A., Tavtigian, S. V., and Bartel, P. L. (1997) *J. Biol. Chem.* **272,** 31941–31944
14. Sharan, S. K., Morimatsu, M., Albrecht, U., Lim, D. S., Regel, E., Dinh, C., Sands, A., Eichele, G., Hasty, P., and Bradley, A. (1997) *Nature* **386,** 804–810
15. Spain, B. H., Larson, C. J., Shihabuddin, L. S., Gage, F. H., and Verma, I. M. (1999) *Proc. Natl. Acad. Sci. U. S. A.* **96,** 13920–13925
16. Tutt, A., Gabriel, A., Bertwistle, D., Connor, F., Paterson, H., Peacock, J., Ross, G., and Ashworth, A. (1999) *Curr. Biol.* **9,** 1107–1110
17. Friedman, L. S., Thistlethwaite, F. C., Patel, K. J., Yu, V. P., Lee, H., Venkitaraman, A. R., Abel, K. J., Carlton, M. B., Hunter, S. M., Colledge, W. H., Evans, M. J., and Ponder, B. A. (1998) *Cancer Res.* **58,** 1338–1343
18. Connor, F., Bertwistle, D., Mee, P. J., Ross, G. M., Swift, S., Grigorieva, E., Tybulewicz, V. L., and Ashworth, A. (1997) *Nat. Genet.* **17,** 423–430
19. Morimatsu, M., Donoho, G., and Hasty, P. (1998) *Cancer Res.* **58,** 3441–3447
20. Marston, N. J., Richards, W. J., Hughes, D., Bertwistle, D., Marshall, C. J., and Ashworth, A. (1999) *Mol. Cell. Biol.* **19,** 4633–4642
21. Jantti, J., Lahdenranta, J., Olkkonen, V. M., Soderlund, H., and Keranen, S.

(1999) *Proc. Natl. Acad. Sci. U. S. A.* **96,** 909–914
22. Futamura, M., Arakawa, H., Matsuda, K., Katagiri, T., Saji, S., Miki, Y., and Nakamura, Y. (2000) *Cancer Res.* **60,** 1531–1535
23. Chan, G. K., Jablonski, S. A., Sudakin, V., Hittle, J. C., and Yen, T. J. (1999) *J. Cell Biol.* **146,** 941–954
24. Ohshima, K., Haraoka, S., Yoshioka, S., Hamasaki, M., Fujiki, T., Suzumiya, J., Kawasaki, C., Kanda, M., and Kikuchi, M. (2000) *Cancer Lett* **158,** 141–150
25. Liu, J., Yuan, Y., Huan, J., and Shen, Z. (2001) *Oncogene* **20,** 336–345
26. Gorlin, J. B., Yamin, R., Egan, S., Stewart, M., Stossel, T. P., Kwiatkowski, D. J., and Hartwig, J. H. (1990) *J. Cell Biol.* **111,** 1089–1105
27. Stossel, T., Condeelis, J., Cooley, L., Hartwig, J., Noegel, A., Schleicher, M., and Shapiro, S. (2001) *Nat. Rev. Mol. Cell Biol.* **2,** 138
28. Ozanne, D. M., Brady, M. E., Cook, S., Gaughan, L., Neal, D. E., and Robson, C. N. (2000) *Mol. Endocrinol.* **14,** 1618–1626
29. Ohta, Y., Suzuki, N., Nakamura, S., Hartwig, J. H., and Stossel, T. P. (1999) *Proc. Natl. Acad. Sci. U. S. A.* **96,** 2122–2128
30. Ohta, Y., and Hartwig, J. H. (1996) *J. Biol. Chem.* **271,** 11858–11864
31. Sharma, C. P., Ezzell, R. M., and Arnaout, M. A. (1995) *J. Immunol.* **154,** 3461–3470
32. Loo, D. T., Kanner, S. B., and Aruffo, A. (1998) *J. Biol. Chem.* **273,** 23304–23312
33. Marti, A., Luo, Z., Cunningham, C., Ohta, Y., Hartwig, J., Stossel, T. P., Kyriakis, J. M., and Avruch, J. (1997) *J. Biol. Chem.* **272,** 2620–2628
34. Vidal, M. (1997) in *The Yeast Two-hybrid System.* (Bartel, P., and Fields, S., eds), pp. 109–147, Oxford University Press, Inc., New York
35. Shen, Z., Peterson, S. R., Comeaux, J. C., Zastrow, D., Moyzis, R. K., Bradbury, E. M., and Chen, D. J. (1996) *Mutat. Res.* **364,** 81–89
36. Shen, Z., Cloud, K. G., Chen, D. J., and Park, M. S. (1996) *J. Biol. Chem.* **271,** 148–152
37. Cunningham, C. C., Gorlin, J. B., Kwiatkowski, D. J., Hartwig, J. H., Janmey, P. A., Byers, H. R., and Stossel, T. P. (1992) *Science* **255,** 325–327
38. Deleted in proof
39. Bertwistle, D., Swift, S., Marston, N. J., Jackson, L. E., Crossland, S., Crompton, M. R., Marshall, C. J., and Ashworth, A. (1997) *Cancer Res.* **57,** 5485–5488
40. Stossel, T. P., Hartwig, J. H., Janmey, P. A., and Kwiatkowski, D. J. (1999) *Biochem. Soc. Symp.* **65,** 267–280
41. Liu, G., Thomas, L., Warren, R. A., Enns, C. A., Cunningham, C. C., Hartwig, J. H., and Thomas, G. (1997) *J. Cell Biol.* **139,** 1719–1733
42. Cunningham, C. C. (1995) *J. Cell Biol.* **129,** 1589–1599
43. Pfaff, M., Liu, S., Erle, D. J., and Ginsberg, M. H. (1998) *J. Biol. Chem.* **273,** 6104–6109
44. Glogauer, M., Arora, P., Chou, D., Janmey, P. A., Downey, G. P., and McCulloch, C. A. (1998) *J. Biol. Chem.* **273,** 1689–1698
45. Critchley, D. R. (2000) *Curr. Opin. Cell. Biol.* **12,** 133–139
46. Fox, J. W., Lamperti, E. D., Eksioglu, Y. Z., Hong, S. E., Feng, Y., Graham, D. A., Scheffer, I. E., Dobyns, W. B., Hirsch, B. A., Radtke, R. A., Berkovic, S. F., Huttenlocher, P. R., and Walsh, C. A. (1998) *Neuron* **21,** 1315–1325
47. Leonardi, A., Ellinger-Ziegelbauer, H., Franzoso, G., Brown, K., and Siebenlist, U. (2000) *J. Biol. Chem.* **275,** 271–278

(Oncogene, Revised MS no. 11199)

Genomic structure of the human BCCIP gene and its role in G1-S transition

Xiangbing Meng, Jingmei Liu, Xu Guo, Zhiyuan Shen[1]

Department of Molecular Genetics and Microbiology
University of New Mexico School of Medicine
915 Camino de Salud, NE
Albuquerque, NM 87131

Running Title: Genomic structure and function of human BCCIP.

Total Figures: 10

Total Tables: 2

Key words: BCCIP, Tok-1, BRCA2, DDX32, bi-directional promoter, G1-arrest, 10q26.1.

Footnotes:

1. To whom correspondence should be sent at email: zshen@salud.unm.edu.
2. The gene symbols of BCCIP and DDX32 used in this report are recommended by the HUGO Gene Nomenclature Committee.
3. Abbreviations: BCCIP: BRCA2 and CDKN1A (Cip1/p21/waf1) Interacting Protein; UROS: Uroporphyrinogen III Synthase; TK: Thymidine Kinase; CAT: Chloramphenicol Acetyl-Transferase; PCNA: Proliferating Cell Nuclear Antigen; BAC: Bacterial Artificial Chromosome; CVD: C-terminal Variable Domain; ICD: Internal Conserved Domain; NAD: N-terminal Acidic Domain; DDX32: DEAD/H (Asp-Glu-Ala-Asp/His) box polypeptide 32; Doc: doxcycline; Noc: nocodazole.
4. Sequences in this report are deposited in GenBank with accession no. AY064247, AY064248, AY064249, and AY064250.

Abstract

Human BCCIPα (Tok-1α) is a BRCA2 and CDKN1A (Cip1, p21) interacting protein. Previous studies showed that BCCIPα can inhibit the growth of certain tumor cells. In this study, we report the genomic structure of the human *BCCIP* gene, which contains 9 exons. Alternative splicing of the 3'-terminal exons produces two isoforms of *BCCIP* transcripts, BCCIPα and BCCIPβ. The *BCCIP* gene is flanked by two genes that are transcribed in the opposite orientation of the *BCCIP* gene. It lies head-to-head and shares a bi-directional promoter with the uroporphyrinogen III synthase (*UROS*) gene. The last 3 exons of *BCCIP* gene overlap the 3'-terminal 7 exons of a DEAD/H helicase-like gene (*DDX32*). Using a matched normal/tumor cDNA array, we identified reduced expression of *BCCIP* in kidney tumor, suggesting a role of *BCCIP* in cancer etiology. In addition, we demonstrate that BCCIPβ also interacts with BRCA2. BCCIPβ inhibits cell growth by delaying G1-S transition, suggesting a functional role of *BCCIP* gene in cell cycle control.

Introduction

The human BCCIPα[2,3] was identified as a BRCA2 and CDKN1A (Cip1/waf1/p21) Interacting Protein (Liu *et al.*, 2001; Ono *et al.*, 2000). A second isoform, BCCIPβ, has also been identified (Liu *et al.*, 2001; Ono *et al.*, 2000). These two isoforms, BCCIPα (322 amino acids) and BCCIPβ (318 amino acids), share 258 identical N-terminal amino acids. Homologues of human BCCIPα and BCCIPβ have been identified from various species, including *C. elegans, S. cerevisiae, A. thaliana*, and mouse. BCCIP proteins contain three distinct domains (Liu *et al.*, 2001): the N-terminal Acidic Domain (NAD), the C-terminal Variable Domain (CVD), and the Internal Conserved Domain (ICD). BCCIPs from various species share no homology in their CVDs. However, their ICDs share significant homology. For example, human and mouse BCCIP share 97% similarity in the ICD, while the yeast and plant BCCIP share about 70% similarity to human BCCIP in their ICD. All the BCCIPs have an N-terminal acidic domain. The evolutionary conservation of the NAD and ICD regions suggests essential functional roles of BCCIP.

BCCIPα and BCCIPβ are nuclear proteins (Liu *et al.*, 2001; Ono *et al.*, 2000). BCCIP gene is abundantly expressed in many tissues, including skeletal muscle, heart, testis, kidney, and brain (Liu *et al.*, 2001; Ono *et al.*, 2000). Ono et al demonstrated that *BCCIPα* and *BCCIPβ* mRNAs reach their highest levels at the G1/S border and remain high in S-phase (Ono *et al.*, 2000), a pattern also shown by *BRCA2, BRCA1, RAD51* and other genes involved in homologous recombinational repair (Bertwistle *et al.*, 1997; Chen *et al.*, 1997; Rajan *et al.*, 1996; Vaughn *et al.*, 1996; Yamamoto *et al.*, 1996). The *BCCIP* gene is mapped to chromosome 10q26.1, loss of heterozygosity of which is associated with many forms of human cancers (Fujisawa *et al.*, 1999; Fujisawa *et al.*, 2000; Ittmann, 1996; Ittmann, 1998; Maier *et al.*, 1998; Peiffer *et al.*, 1995; Petersen *et al.*, 1998; Rasheed *et al.*, 1995; Rasheed *et al.*, 1999; Walker *et al.*, 1995). Some

breast and brain cancer cell lines exhibit reduced BCCIPα protein expression (Liu *et al.*, 2001). Over-expression of BCCIPα moderately inhibits certain breast cancer and brain cancer cell growth (Liu *et al.*, 2001).

Due to its interaction with BRCA2 and p21, it is anticipated that *BCCIP* is a gene of importance in cancer etiology, thus warrant further characterization. Here, we report the genomic organization of *BCCIP*, alternative splicing that produces two isoforms of *BCCIP* transcript, a bi-directional promoter that drives *BCCIP* gene expression, and expression levels of BCCIP transcripts in 68 cases of human cancer. We further demonstrated that BCCIPβ also interacts with BRCA2, and overexpression of BCCIPβ strongly inhibits cell growth and arrests cells at G1-phase.

Results and discussion

Genomic organization of BCCIP gene

We screened the human RPCI.11 BAC library array (Research Genetics), and obtained 2 BAC clones (569M14 and 634J20) that contain the *BCCIP* gene. We then performed direct DNA sequencing of the BAC clones (see Materials and Method) and identified the intron/exon boundary sequences. A sequence search of the human genome High Throughput Genomic sequence database identified a BAC clone (RP11-124H7) of chromosome 10 that contains the *BCCIP* gene (GenBank accession No. 16044807). Combining the sequence information from this entry and our own data, we composed a sequence segment of 70 kb (GenBank accession no. AY064247[4]), which was used to produce the diagram of the genomic organization at the BCCIP gene region (Figure 1).

The *BCCIP* gene contains 9 exons (Figure 1). At its 5'-end, the *BCCIP* gene abuts the uroporphyrinogen III synthase (*UROS*) gene (Aizencang *et al.*, 2000a) in a "head-to-head" manner. There is a 278 bp intergenic region between the *BCCIP* and *UROS*. The three 3'-terminal exons of *BCCIP* overlap with the seven 3'-terminal exons of a DEAD/H helicase like gene, *DDX32*[2] (GenBank Accession No. AY064250 and AF427340), which is transcribed on the opposite strand of the *BCCIP* coding strand.

Alternative splicing of BCCIP gene

All *BCCIP* exon-intron boundary sequences conform the GT-AG rule (Table 1). Comparison of the genomic sequence with the cDNA of BCCIPα and BCCIPβ (GenBank Accession No. AY06248 and AY06249) revealed that BCCIPα and BCCIPβ represent 3'-terminal alternative splicing products of a single human *BCCIP* gene (Figure 2). Exons 1-6 encode for the N-terminal shared 258 amino acids of BCCIPα and BCCIPβ isoforms, including the NAD (exon 1) and the ICD (exons 2-6). Exon 7 is specifically spliced to encode the CVD of BCCIPβ, and exons 8 and 9 encode the CVD of BCCIPα (Figure 2).

This 3'-terminal alternative splicing of BCCIP is analogous to that of Calcitonin/Calcitonin Gene-Related Peptide gene, one of the first examples of mammalian alternatively spliced genes (Amara *et al.*, 1984; Amara *et al.*, 1982; Lou & Gagel, 1998; Yeakley *et al.*, 1993). In the case of Calcitonin, alternative splicing is used to generate tissue specific transcripts. Ono et al reported that BCCIPα isoform directly binds to p21 while BCCIPβ does not (Ono *et al.*, 2000). However, we have found that both BCCIPα and BCCIPβ isoforms interact with BRCA2 (to be presented in

Figure 7). Therefore, it remains to be determined whether the alternative splicing is regulated to generate two isoforms of BCCIP proteins with specific biological activities.

BCCIP expression is driven by a bi-directional promoter

It is common for mammalian cells to use a shared bi-directional promoter to activate the transcriptions of two neighboring genes on the opposite orientations (Ame *et al.*, 2001; Chinenov *et al.*, 2000; Suen & Goss, 1999; Xu *et al.*, 1997). For example, a 218-229 bp region is responsible for the transcription of BRCA1 and the flanking NBR2 gene (Suen & Goss, 1999; Xu *et al.*, 1997). Since *BCCIP* and *UROS* are separated by 277 bases, and these genes are transcribed on opposite strands (Figures 1), we sought to determine whether the intergenic region between BCCIP and UROS contains promoter activities for both genes.

We constructed eight reporter plasmids by replacing the TK promoter in pTK-CAT (Figure 3A) with different DNA fragments of the intergenic region between BCCIP and UROS in both orientations (Figure 3C). These CAT constructs were co-transfected into COS7 cells with the pCH110 plasmid (Figure 3B), which was used as an internal control for the transfection since it expresses β-Gal reporter gene constitutively from a SV40 promoter. The ratio of CAT activity to β-Gal activity represents the relative promoter activity in the CAT constructs. The pTK-CAT plasmid (Figure 3A) was used as a positive control, and a CAT plasmid without any promoter sequence was used as a negative control. As Figure 3D shows, the 277 bp region between the *UROS* and *BCCIP* contains promoter activities in both orientations at a level comparable to the TK promoter. Therefore, BCCIP and UROS genes share an intergenic bi-directional promoter for their expression. We further determined that an 80 bp of sequence (contained in fragments UROS3 and BCCIP-5) proximate to the UROS gene has basal transcription activity in both directions.

However, the transcription activity of this short region in the BCCIP orientation is significantly reduced (compare BCCIP-5 and full-length BCCIP fragments). Extending the length of promoter region from bases 1-80 to bases 1-137 significantly increase the transcription activity (compare BCCIP-5 with BCCIP-6). But, further extending the promoter from bases 1-137 to bases 1-207 reduces the transcription activity (compare BCCIP-6 to BCCIP-7). Lastly, the BCCIP-3 fragment (bases 81-277) has significant lower transcription activity than all others. These data suggest that there may be positive and negative regulatory elements between bases 81-277 that play roles for the fine-tuning of BCCIP gene expression. A putative enhancer element between bases 80-139 was identified by sequence analysis (see Figure 4), but no negative regulatory element was seen by the same analysis (see Material and Method for details of promoter sequence analysis). We further identified several potential binding sites of transcription factors in the promoter region, including SP1, YY1, AP-1, AP2, and PEA2 (Figure 4).

Expression of BCCIP in human tissues

We tested the BCCIP mRNA level in several human tissues. As Figure 5 shows, BCCIP mRNA is highly expressed in skeletal muscle and heart tissues, consistent with previous reports (Liu *et al.*, 2001; Ono *et al.*, 2000). We also found an abundant expression of BCCIP mRNA in kidney, liver and placenta tissues. The high levels of expression of BCCIP in skeletal muscle, liver, and heart are consistent with that of the housekeeping *UROS* gene that is transcribed from the same bi-directional promoter (Aizencang *et al.*, 2000a; Aizencang *et al.*, 2000b).

BCCIP expression in human cancers

BCCIPα protein interacts with BRCA2 and p21, which participate in DNA repair and cell cycle control. *BCCIP* gene is also located in chromosome 10q26.1, which is associated with many human cancers (Fujisawa *et al.*, 1999; Fujisawa *et al.*, 2000; Ittmann, 1996; Ittmann, 1998; Maier *et al.*, 1998; Peiffer *et al.*, 1995; Petersen *et al.*, 1998; Rasheed *et al.*, 1995; Rasheed *et al.*, 1999; Walker *et al.*, 1995). We previously measured the BCCIP protein levels in 27 cancer cell lines (Liu *et al.*, 2001), and found that 3 out of the 9 brain tumor cell lines, 3 out of the 7 breast cancer cell lines, and 2 out of 4 endometrial cancer cell lines exhibited reduced BCCIPα protein levels. These data suggest a potential role of BCCIPα in cancer etiology. We further measured BCCIP mRNA expression in 68 cases of human tumors (Table 2). This was done with a Matched Tumor/Normal Expression Array (see Material and Methods for details). Each cDNA on this array is directly derived from mRNA of human tumor samples with a matched normal tissue. As certified by the manufacturer, the cDNA levels on the array were normalized to cell type within the same tissue and directly reflect the relative abundance of mRNA levels between tumor and normal tissues of the same organs. Thus it can be used to compare the relative expression level of a specific gene between the normal and tumor of the same tissue. We used a cDNA fragment from exon 7 as the BCCIPβ-specific probe, and a cDNA fragment containing exons 8 and 9 as the BCCIPα specific probe, and analyzed the expression levels of BCCIPα and BCCIPβ in these tumor samples. The levels of ubiquitin mRNA were used as the internal control as recommended by the manufacturer of the cDNA array.

Figure 6 shows the relative BCCIPα (6A) and BCCIPβ (6B) mRNA levels in the tumor samples. A major observation is that the majority of kidney tumors exhibit reduced BCCIPα and BCCIPβ mRNA expression. The average BCCIPα and BCCIPβ mRNA levels from the 15 kidney tumors are significantly lower than their matched normal tissues ($p<0.005$, t-test). In addition, 1 of

9 breast cancers and 1 of the 15 kidney cancers lack detectable BCCIPβ mRNA, 2 out of 11 colon cancer and 1 out of 7 uterus cancer have 10-100 fold reduction of BCCIPβ mRNA levels as shown in Figure 6B. These data further implicate BCCIP in cancer etiology.

Interaction between BCCIPβ and BRCA2

We initially identified the interaction between the BCCIPα isoform and BRCA2 (Liu *et al.*, 2001). We further mapped the BRCA2-interacting domain to amino acids 59-167 of BCCIP (data not shown). Since this BRCA2-interacting domain is identical in BCCIPα and BCCIPβ, we tested whether BCCIPβ also interacts with BRCA2 using Co-IP (Figure 7). In all the Co-IP experiments, the Benzonase nuclease (Novagene) was used to treat the protein samples to eliminate the interference of DNA/RNA on protein complex formation. We co-precipitated endogenous BCCIPα and BCCIPβ with anti-BRCA2 antibodies in HeLa cells (Figure 7A). To confirm this result, Myc-tagged BCCIPα and BCCIPβ were expressed in HeLa cells and precipitated with anti-Myc antibodies (Figure 7B). RAD51 was used as positive control, and UBC9 and RAD52 were used as negative controls. As expected, endogenous BRCA2 co-precipitated with RAD51, BCCIPα, and BCCIPβ, but not RAD52 or UBC9. These data confirm that BCCIPβ also interacts with BRCA2.

Growth inhibition conferred by overexpression of BCCIPβ

We have reported that overexpression of BCCIPα moderately inhibits certain breast cancer cell growth (Liu *et al.*, 2001). These data were obtained from stable cell lines constitutively overexpressing BCCIPα. To test whether BCCIPβ also inhibits cell growth, we attempted to construct stable cell lines constitutively overexpressing BCCIPβ but failed, suggesting that

BCCIPβ strongly inhibits cell growth. To confirm this prediction, we cloned BCCIPα and BCCIPβ into a mammalian expressing vector with puromycin selection marker, transfected equal amounts of those vectors into HeLa, and HT1080 fibrosarcoma cells, selected the transfected cells in puromycin for two weeks, and stained to visualize the grown cells. As shown in Figure 8A, compared to cells transfected with control vector, there are less cells grown when transfected with BCCIPα and no cells grown when transfected with BCCIPβ, although approximately equal amount of BCCIPα and BCCIPβ proteins were detected shortly after the transfection (Figure 8B). These data suggest that BCCIPβ has stronger inhibition on cell growth than BCCIPα. Furthermore, we constructed a doxcycline(Doc)-inducible BCCIPβ overexpressing cell line using the pTet-ON and pREV-TRE vectors (See Material and Methods) in HT1080 cells, designated HT1080/TetOn-BCCIPβ (Figure 9A). As shown in Figure 9B, when BCCIPβ overexpression is induced, the growth of HT1080 cells is severely inhibited. These data confirm that BCCIPβ also inhibits cell growth.

Delayed G1-S transition induced by overexpression of BCCIPβ

To investigate the mechanism by which BCCIPβ inhibits cell growth, we used flowcytometry to analyze the nuclear DNA content of the cells after BCCIPβ is overexpressed, and observed a shift of cell cycle distribution to G1-phase (data not shown), suggesting a G1-delay. To confirm this, we treated cells with 10μg/ml of nocodazole (Noc) to block cells at M phase so that no new G1 cells can be generated. Therefore, the gradual disappearance of the G1 peak can be used to evaluate the dynamics of the G1-S transition. At several time points after Noc treatment, cells were collected and analyzed for DNA content by flow cytometry. As shown in Figure 10, the G1 phase peak nearly disappeared for the control cells within 8-16 hours (columns 1 and 2), but a

significant amount of BCCIPβ-overexpressing cells remains in G1 phase, even 24 hours after the Noc blocking (column 3). These data suggest that BCCIPβ suppresses cell growth by inhibiting G1-S transition.

In summary, we have delineated the genomic organization of the human *BCCIP* gene and identified a bi-direction promoter for *BCCIP* and *UROS* expression. Our results show that BCCIPα and BCCIPβ are products of 3'-terminal alternative splicing of a single gene located at chromosome 10q26.1, and that BCCIP expression is reduced in certain tumors. We further identified a functional role of BCCIPβ in cell growth control and G1-S transition.

Materials and methods

Isolation and sequencing of BAC clones

The BCCIPα cDNA isolated previously (Liu *et al.*, 2001) was used as a probe to screen the RPCI11 BAC library (Research Genetics, Huntsville, AL). The BAC clones (569M14 and 634J20) were identified and BAC DNAs were purified according to protocols provided by the vendor. Primers at the 5'- and 3'-ends of cDNA were initially used to directly sequence the BAC DNA using the BigDye^{Tm} Terminator RR Mix kit (PE Applied Biosystems, Foster City, CA) and an automated DNA sequencer. These sequence data revealed the intron/exon junctions of the first and last exons of BCCIP. Subsequently, new primers from the neighboring exons and introns were synthesized to sequence the BAC clones (primer walking). Thus, the sequences of intron/exon junctions and the promoter were identified. We searched the human genome High Throughput Genomic sequence database, and identified a sequence entry based on chromosome 10 BAC clone RP11-124H7 containing the BCCIP gene (GenBank accession no. 16044807). Combining the

sequence information from this entry and our own sequence data, a 70 kb segment of genomic sequence that contains the entire BCCIP was composed and submitted to GenBank (accession no. AY064247).

Analysis of the BCCIP promoter

The Gal4 binding sites in the plasmid pGAL4-TKCAT (Shi *et al.*, 1991) were removed by Hind III and Xba I digestion and religation, resulting a new reporter plasmid designated pTK-CAT. A panel of CAT reporter plasmids was constructed by replacing the TK promoter in pTK-CAT with various regions of the putative BCCIP promoter. To test promoter activities, 4μg of the CAT reporter plasmids were co-transfected into COS7 cells, together with 0.2μg pCH110 (Amersham, Piscataway, NJ), which expresses β-Gal protein from a constitutive SV40 promoter. Forty-eight hours after transfection, whole cell extracts were prepared, and CAT and β-Gal activities were measured by CAT and β-Gal ELISA kits (Boehringer Mannheim, Indianopolis, IN) and the SPECTRAmax Plus^{384} microplate spectrophotometer with the SOFTmax PRO data analysis program package (Molecular Devices Corporation, Sunnyvale, CA). The ratio of concentrations between CAT to β-gal represents the transcription activity of the promoters in a specific CAT reporter plasmid. Putative transcription factor-binding sites were identified by scanning the promoter sequence with the Tfsitescan program provided by the Institute of Transcriptional Informatics (Pittsburg, PA) at the website http://www.ifti.org/cgi-bin/ifti/tfsitescan.pl. Only the putative sites with significant Expectation values were presented.

Northern Blot Analysis

A pre-made multiple-tissue Northern blot was purchased from Clontech (Palo Alto, CA). This blot was hybridized with ^{32}P-dCTP labeled cDNA of exons 1-6 of BCCIP according to the protocol provided. A β-Actin probe was used as a control for the hybridization as suggested by the manufacturer.

Expression of BCCIP in human tumors

To measure the mRNA expression of BCCIP gene in human tumors, a Matched Tumor/Normal Expression Array was purchased (Clontech, Catalog No. 7840-1). The amount of cDNA on this array was normalized to levels of three different housekeeping genes and cell types within the same tissue, and thus reflect the relative abundance of mRNA levels in these tissues. We labeled exon 7 with ^{32}P-dCTP and hybridized with the array to detect BCCIPβ mRNA, and exons 8 and 9 to detect BCCIPα level. The hybridized array was scanned with a Molecular Dynamics Phosphorimager, and the SPOTFINDER™ software provided. The signal from each normal and tumor samples was normalized to the mRNA levels of ubiquitin in the same sample as recommended by the manufacturer.

Cell culture and construction of doxcycline (Doc)-inducible BCCIPβ expression.

HeLa and HT1080 cells were cultured in DEME and αMEM (Biowhiter) respectively with 10% fetal calf serum, 1% Penicillin/Streptomycin, and 2mM glutamine. Doc-inducible overexpression of BCCIPβ in HT1080 cells were established by pRevTet-ON system and the RetroPack™ PT67 packaging cell lines according to the manuals provided by the manufacturer (Clontech, Palo Alto,

CA). This cell line, designated HT1080/TetOn-BCCIPβ, was maintained in the absence of Doc. Doc-inducible BCCIPβ expression was confirmed by anti-BCCIP immunoblot (Figure 9A).

Co-immunoprecipitation (Co-IP) and Western blot

To co-precipitate endogenous BCCIP with endogenous BRCA2, cells were lysed in lysis buffer (50mM HEPES pH7.6, 250mM NaCl, 5mM EDTA, 0.1% Nonidet P-40). This lysed protein solution was treated with Benzonase nuclease (Novagene, Madison, WI) to digest nucleic acids. Two milligrams of protein were incubated with 4μg of anti-BRCA2 antibody (Oncogene Research Product, Boston, MA) for 1.5hrs, Protein A plus G beads were added for additional 2hrs. Beads were collected and washed ten times in lysis buffer. Then 2X SDS sample buffer was added and heated at 55^0C for 10 minutes to elute the precipitated proteins. The eluted proteins were subjected to Western blot (see bellow).

To co-precipitate the endogenous BRCA2 with Myc-tagged proteins, BCCIPs, RAD51, RAD52, UBC9 were cloned into pMyc-CMV vector to tag them with the Myc epitope. Plasmids were transfected into HeLa cells using GenePorter transfection reagent (GeneTherapy Systems). Forty-eight hours after transfection, cells were collected, treated with lysis buffer, sonicated, and centrifuged for 10 minutes at 10,000 rpm. The supernatant (whole cell lysate) was treated with Benzonase and used for immunoprecipitation. Forty microliters of anti-Myc affinity bead (Clontech, Palo Alto, CA) was incubated with 1 mg of whole cell lysate at 4^0 C on a rocker for 20 minutes. The matrix was then washed ten times. Proteins retained on the beads were eluted with 2X SDS sample buffer by boiling for five minutes. The eluted proteins were subjected to Western blot (see bellow).

Eluted proteins from the CO-IP and other protein samples were resolved by 5% or 12% PAGE gel. Western blotting was performed using anti-Myc (Clontech, Palo Alto, CA), anti-BRCA2 (Oncogene Researcher Products, Boston, MA), anti-BCCIP (Liu *et al.*, 2001), anti-HA (Clontech, Palo Alto, CA), and anti-actin (Sigma, St. Louis, MO) antibodies.

DNA content based cell cycle analysis

The method originally described by Vindelov et al was adapted to stain nuclear DNA for flowcytometry analysis (Vindelov *et al.*, 1983). Briefly, cells were trypsinized, washed with PBS and fixed with 70% ethanol. Then cells were pelleted, washed with PBS and suspended in 200 µl of citrate buffer (250 mM Sucrose, 0.05% DMSO, 40 mM Trisodium citrate, ph7.6). Nine hundred microliters of Solution A [0.003% tripsin in stock buffer (3.4 mM Trisodium citrate, 0.1% Nonidet P 40, 1.5 mM Spermine tetrahydrochloride, 0.5 mM Trizma, pH 7.6)] were added and cells were incubated at room temperature for 10 minutes. Afterwards, 750 µl Solution B (0.025% Trypsin inhibitor, 0.01% Ribonuclease A in stock buffer) was added for another incubation of 30 minutes at room temperature. Then 750 µl of Solution C (0.0416% Propidium iodide, 3.3 mM Spermine tetrahydorchloride in stock buffer) was added to the cells and analyzed by flowcytometry. In each assay, 20,000 cells were collected by FACScan (Becton Dickinson) and analyzed by CellQuest software provided.

Acknowledgments

We thank Mark Brenneman (University of New Mexico) for critical reading of the manuscript. This research was supported by National Institute of Health NIEHS grant ES08353 and by the US

Army Medical Research and Materiel Command grant DAMD17-98-1-8198. Its contents are solely the responsibility of the authors and do not necessarily represent the official views of these funding agencies.

References

Aizencang, G., Solis, C., Bishop, D.F., Warner, C. & Desnick, R.J. (2000a). *Genomics*, **70,** 223-31.

Aizencang, G.I., Bishop, D.F., Forrest, D., Astrin, K.H. & Desnick, R.J. (2000b). *J Biol Chem*, **275,** 2295-304.

Amara, S.G., Evans, R.M. & Rosenfeld, M.G. (1984). *Mol Cell Biol*, **4,** 2151-60.

Amara, S.G., Jonas, V., Rosenfeld, M.G., Ong, E.S. & Evans, R.M. (1982). *Nature*, **298,** 240-4.

Ame, J.C., Schreiber, V., Fraulob, V., Dolle, P., de Murcia, G. & Niedergang, C.P. (2001). *J Biol Chem*, **276,** 11092-9.

Bertwistle, D., Swift, S., Marston, N.J., Jackson, L.E., Crossland, S., Crompton, M.R., Marshall, C.J. & Ashworth, A. (1997). *Cancer Res*, **57,** 5485-8.

Chen, F., Nastasi, A., Shen, Z., Brenneman, M., Crissman, H. & Chen, D.J. (1997). *Mutat Res*, **384,** 205-11.

Chinenov, Y., Coombs, C. & Martin, M.E. (2000). *Gene*, **261,** 311-20.

Fujisawa, H., Kurrer, M., Reis, R.M., Yonekawa, Y., Kleihues, P. & Ohgaki, H. (1999). *Am J Pathol*, **155,** 387-94.

Fujisawa, H., Reis, R.M., Nakamura, M., Colella, S., Yonekawa, Y., Kleihues, P. & Ohgaki, H. (2000). *Lab Invest*, **80,** 65-72.

Ittmann, M. (1996). *Cancer Res*, **56,** 2143-7.

Ittmann, M.M. (1998). *Oncol Rep*, **5,** 1329-35.

Liu, J., Yuan, Y., Huan, J. & Shen, Z. (2001). *Oncogene*, **20,** 336-345.

Lou, H. & Gagel, R.F. (1998). *J Endocrinol*, **156,** 401-5.

Maier, D., Zhang, Z., Taylor, E., Hamou, M.F., Gratzl, O., Van Meir, E.G., Scott, R.J. & Merlo, A. (1998). *Oncogene*, **16,** 3331-5.

Ono, T., Kitaura, H., Ugai, H., Murata, T., Yokoyama, K.K., Iguchi-Ariga, S.M. & Ariga, H. (2000). *J Biol Chem*, **275,** 31145-54.

Peiffer, S.L., Herzog, T.J., Tribune, D.J., Mutch, D.G., Gersell, D.J. & Goodfellow, P.J. (1995). *Cancer Res*, **55,** 1922-6.

Petersen, S., Rudolf, J., Bockmuhl, U., Gellert, K., Wolf, G., Dietel, M. & Petersen, I. (1998). *Oncogene*, **17,** 449-54.

Rajan, J.V., Wang, M., Marquis, S.T. & Chodosh, L.A. (1996). *Proc Natl Acad Sci U S A*, **93,** 13078-83.

Rasheed. B.K., McLendon, R.E., Friedman, H.S., Friedman, A.H., Fuchs, H.E., Bigner, D.D. & Bigner, S.H. (1995). *Oncogene*, **10,** 2243-6.

Rasheed, B.K., Wiltshire, R.N., Bigner, S.H. & Bigner, D.D. (1999). *Curr Opin Oncol*, **11,** 162-7.

Shi, Y., Seto, E., Chang, L.S. & Shenk, T. (1991). *Cell*, **67,** 377-88.

Suen, T.C. & Goss, P.E. (1999). *J Biol Chem*, **274,** 31297-304.

Vaughn, J.P., Cirisano, F.D., Huper, G., Berchuck, A., Futreal, P.A., Marks, J.R. & Iglehart, J.D. (1996). *Cancer Res*, **56,** 4590-4.

Vindelov, L.L., Christensen, I.J. & Nissen, N.I. (1983). *Cytometry*, **3,** 323-7.

Walker, G.J., Palmer, J.M., Walters, M.K. & Hayward, N.K. (1995). *Genes Chromosomes Cancer*, **12,** 134-41.

Xu, C.F., Brown, M.A., Nicolai, H., Chambers, J.A., Griffiths, B.L. & Solomon, E. (1997). *Hum Mol Genet*, **6,** 1057-62.

Yamamoto, A., Taki, T., Yagi, H., Habu, T., Yoshida, K., Yoshimura, Y., Yamamoto, K., Matsushiro, A., Nishimune, Y. & Morita, T. (1996). *Mol Gen Genet*, **251,** 1-12.

Yeakley, J.M., Hedjran, F., Morfin, J.P., Merillat, N., Rosenfeld, M.G. & Emeson, R.B. (1993). *Mol Cell Biol*, **13,** 5999-6011.

Table 1. BCCIP gene exon/intron junction sequences.

Exon	3'-splice acceptor sequence	Location	Exon length (bp)	Location	5'-splice donor sequence	Intron size (BCCIPα) (bp)	Intron size (BCCIPβ) (bp)
1	(Promoter)GCAGGCGCAGTG	7358	188	7546	GTCATTGACGAGgtgagaaggaca	2868	2868
2	tgttatttacagGAAGTGAATATT	10414	75	10489	TTACTGCAGCAGgtattgtctttt	892	892
3	tcctccttttagCTTTTTCTAAAG	11381	81	11462	AGTGTGATTAAGgtaagtaggata	2923	2923
4	cttttaaaatagCAAACGGATGTT	14385	90	14475	ACTGAAAGAAAGgttggtttcact	768	768
5	tttgctttctagGGTACCCAGTGT	15243	188	15431	CCAGCAGCTTCAgtaagagattct	2164	2164
6	tgtgccttgcagGAAAGAACTGGC	17595	175	17770	TTTTTCTATGAGgtaagactatcc	7309	2157
7	tatttggtttagAAGGCAATTCTC	19927	448	20375	ATTTTAAAATAAtatacacagtgt (PolyA)	N/A	Poly A
8	ctattccggcagGAGCAGGGAAAA	25078	76	25154	TACAGCACAATGgttggtctgttc	11795	
9	ttttccttacagGTGGTTCACGGG	36949	456	37405	ATAAAGGGGCTAtcaaaaaaatcc (PolyA)	Ploy A	

Table 2, number of tumor cases analyzed for BCCIP gene expression	
Tumor Type	No. of Cases
Kidney	15
Colon	11
Breast	9
Stomach	8
Uterus	7
Rectum	7
Prostate	3
Ovary	3
Lung	3
Cervix	1
Small intestine	1
Total number of cases	68

Figure legends

Figure 1. Genomic organization at the BCCIP locus. A region of 70 kb of double stranded DNA at the *BCCIP* locus is illustrated in scale. There are at least three genes in this region. The boxes indicate the location of exons. The *BCCIP* gene contains 9 exons (top strand) that spans approximately 30 kb. On the opposite (bottom) strand of the DNA, the *UROS* gene and a DEAD/H helicase like gene (*DDX32*) are transcribed. Exons 2 and 3 of UROS are too close to each other and therefore represented by a single box. Similarly, exons 5 and 6 of the *DDX32* gene are separated by a very small intron and therefore are also represented by a single box. The *UROS* and *BCCIP* gene are separated by a 277 bp intergenic region. Additionally, the 3-terminal exons of *BCCIP* and the *DDX32* gene overlap with each other.

Figure 2. 3'-terminal alternative splicing produces two forms of BCCIP mRNA transcripts. The BCCIPα isoform (top panel) results from the splicing of exons 1, 2, 3, 4, 5, 6, 8, and 9. The BCCIPβ isoform (bottom panel) results from the splicing of exons 1, 2, 3, 4, 5, 6, and 7. The polyA addition signals of the α and β transcripts are coded in exons 9 and 7 respectively. The amino acid residues coded by each exon are indicated in the top and bottom panels. Amino acid 200 is coded by the junction between exons 5 and 6, and amino acid 283 of the α isoform is coded by the junction between exons 8 and 9.

Figure 3. BCCIP promoter analysis. Panel A illustrates the expression cassette of a CAT reporter (pTK-CAT) driven by a TK promoter. The TK promoter can be replaced by various promoter sequences (Panel C) to generate a panel of new CAT reporter plasmids. Panel B is the

expression cassette of the reference plasmid (pCH110) that expresses the β-gal gene from the SV40 promoter, which serves as an internal control for transfection. Panel C illustrates eight promoter segments and their orientations that were used to replace the TK promoter in pTK-CAT to generate a panel of new CAT reporter plasmids. Panel D illustrates the promoter activity of the segments in Panel C. The transcription activity is normalized to the reference β-gal activity expressed from pCH110, which was co-transfected with the CAT reporters. A CAT reporter without any promoter (Shown as "none") was used as negative control, and the TK promoter was used as positive control. Shown are the averages of 4 experiments. The error bars indicate standard errors of the means.

Figure 4. Potential binding sites for transcription factors in the BCCIP promoter. The promoter sequence is illustrated in the BCCIP orientation. The putative binding sites for the transcription factors are underlined. Three sites bordering the promoter segment used in Figure 3C are also indicated.

Figure 5. BCCIP expression in various human tissues. Northern blot of a multiple tissue mRNA membrane. Panel A indicates the BCCIP mRNA levels, and panel B indicates the β-actin levels in these tissues.

Figure 6. BCCIP expression in tumor tissues. Shown are the BCCIPα (panel A) and BCCIPβ (panel B) mRNA levels in tumor and matched normal tissues. The cancer types are labeled on the top of panel A. Relative expression level was normalized to ubiquitin mRNA, and grouped

according to tissue type. One case of kidney and one case of breast cancer have BCCIPβ signals below the background, therefore the values of these two cases were not plotted in panel B.

Figure 7. Interactions between BRCA2 and BCCIP.

A. Co-IP of endogenous BCCIPα and BCCIPβ with endogenous BRCA2. The endogenous BRCA2 proteins were immunoprecipitated with mouse anti-BRCA2 antibodies (lane 4). A non-specific mouse IgG and beads without antibody were used as negative controls (lanes 3 and 2). The whole cell extract (lanes 1) and precipitated proteins (Lanes 2-4) were blotted with anti-BRCA2 antibodies (top panel) and rabbit anti-BCCIP antibodies (bottom panel).

B. Co-IP of endogenous BRCA2 with myc-tagged BCCIPα and BCCIPβ. Myc-tagged proteins (indicated on the top of the figure) were expressed in HeLa cells, and precipitated with anti-Myc antibodies. The precipitated Myc-tagged proteins are shown in the top panel. The co-precipitated endogenous BRCA2 protein (bottom panel) were detected by anti-BRCA2 antibodies. For more details, see text.

Figure 8. Expressions of BCCIP inhibit growth of HeLa and HT1080 cells.

A. Inhibition of cell growth by BCCIPα and BCCIPβ. Half million of HeLa and HT1080 cells were transfected with 10 μg of vectors expressing HA-BCCIPα (column 2) or HA-BCCIPβ (column 3). Stably transfected cells were selected by antibiotics, and stained by crystal violet after two weeks. An empty vector (column 1) was used as control. This figure shows that although equal amount of vector was used, no stable cells expressing BCCIPβ can be obtained, and less cells expressing BCCIPα were obtained in comparison with empty vector control.

B. Expression of BCCIPα and BCCIPβ in HeLa and HT1080 cells shortly after the transfection. Forty eight hours after the transfection, equal amount of proteins from a set of the same transfection as described in panel A was analyzed for HA-BCCIPα and HA-BCCIPβ expression by anti-HA antibody (top Panel). Anti-actin antibody (bottom panel) was used to illustrate that approximately equal amount of total proteins was loaded to each of the samples.

Figure 9. Induced-BCCIPβ overexpression inhibits the growth of HT1080 cells.

A. Doc-inducible BCCIPβ expression in HT1080 cells. HA-tagged BCCIPβ were cloned into pREV-TRE (Clontech), which was introduced via retroviral infections into HT1080 cells that had been previously transfected with pTet-On vector, resulting in a doxycycline (Doc)-inducible HA-BCCIPβ expressing cell line, designated HT1080/TetOn-BCCIPβ. Shown in top panel is the exogenously expressed HA-BCCIPβ levels detected by anti-HA antibodies. The same blot was re-blotted with anti-actin (bottom panel) to show that equal amounts of proteins were loaded for each of the samples. As shown, HA-BCCIPβ was significantly induced by Doc in this cell line (lane 3) as compared to non-induced condition (lane 2). The control cell line (lane 1) is the wild type HT1080 cells treated with Doc.

B. Induced BCCIPβ expression inhibits cell growth. Shown are the growth curves of a wild type HT1080 cells (triangle), HT1080/TetOn-BCCIPβ cells with non-induced BCCIPβ (square) expression, and HT1080/TetOn-BCCIPβ cells with induced BCCIPβ expression (circle).

Figure 10. Induced-BCCIPβ overexpression delays G1-S transition. HT1080/TetOn-BCCIPβ cells as in Figure 9 were treated with Doc for 3 day to induce BCCIPβ overexpression (column 3). Control groups are wild type HT1080 treated with Doc (column 1) and mock-treated

HT1080/TetOn-BCCIPβ (column 2). Then, 10μg/ml of nocodazole (Noc) was added to the cells. Various times after continuous Noc treatment (labeled on the left), cells were collected for DNA content analysis using flowcytometry. The gradual disappearance of the G1-peak represents the transition of G1-phase cells into S-phase.

Meng, et al. Figure 1.

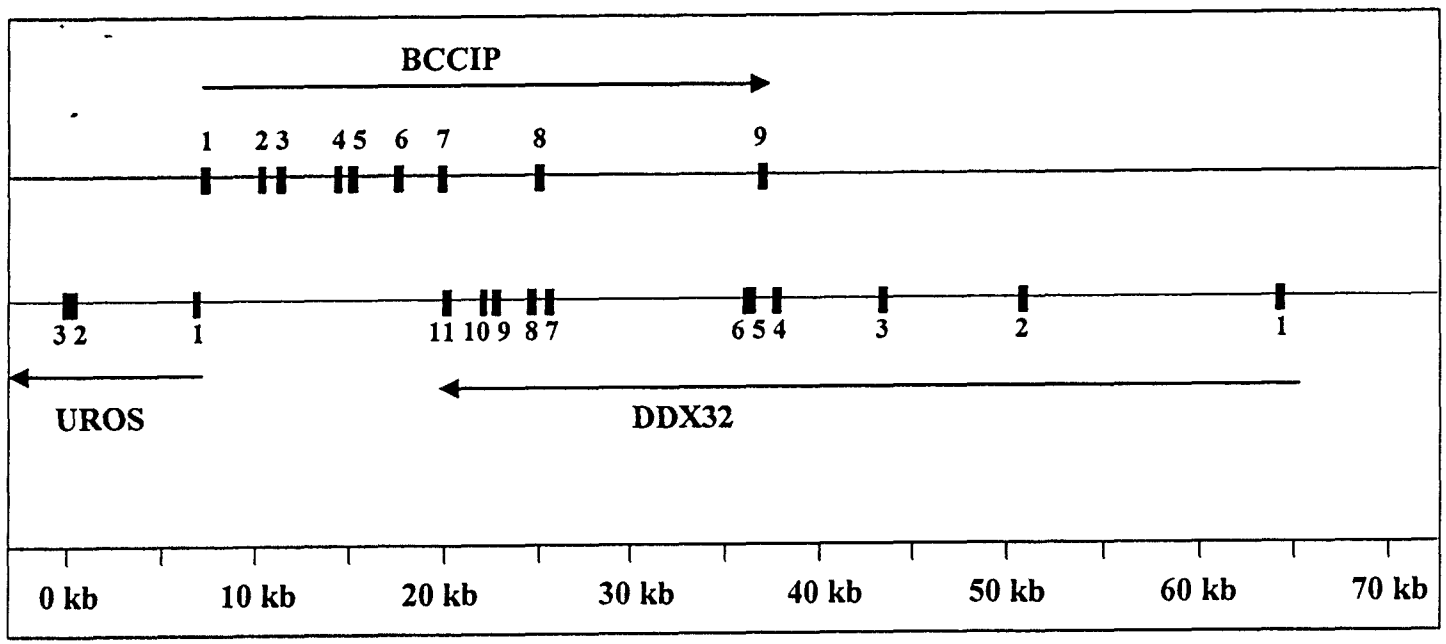

Meng, et al. Figure 2.

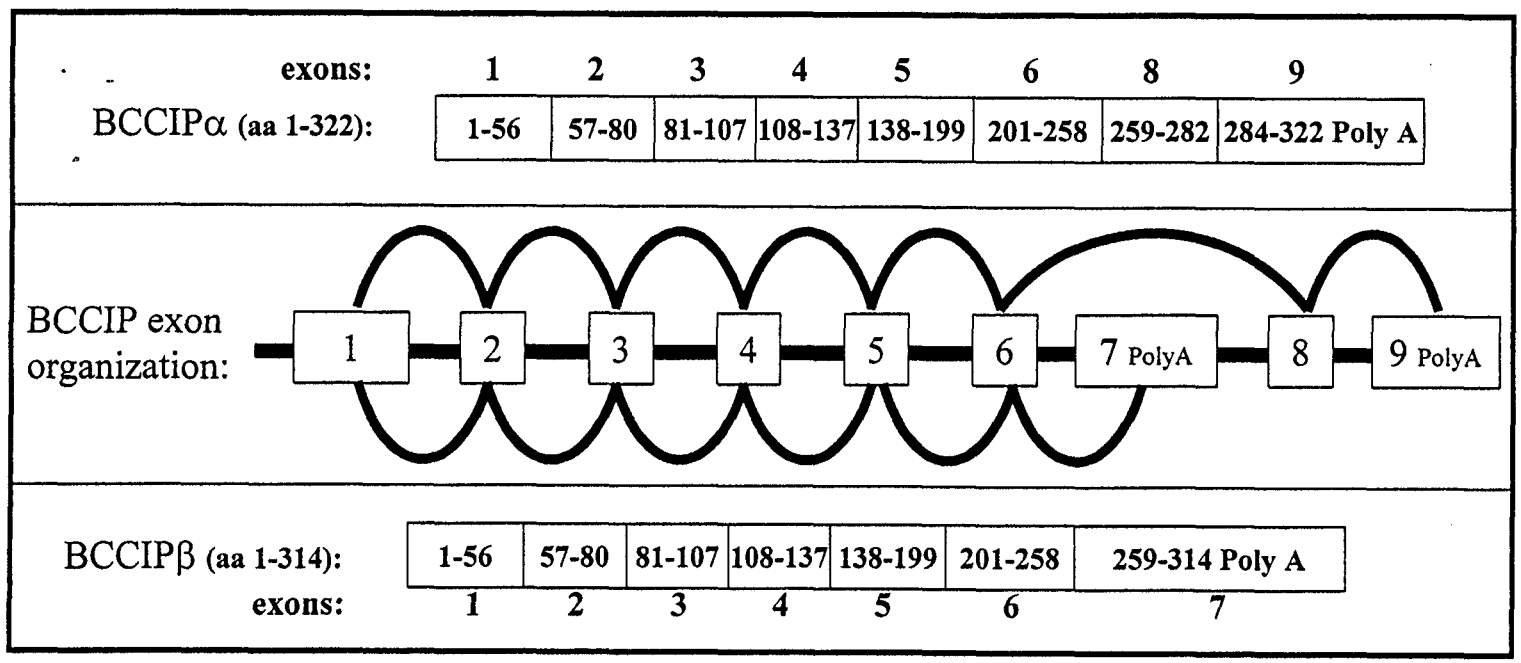

Meng, et al. Figure 3.

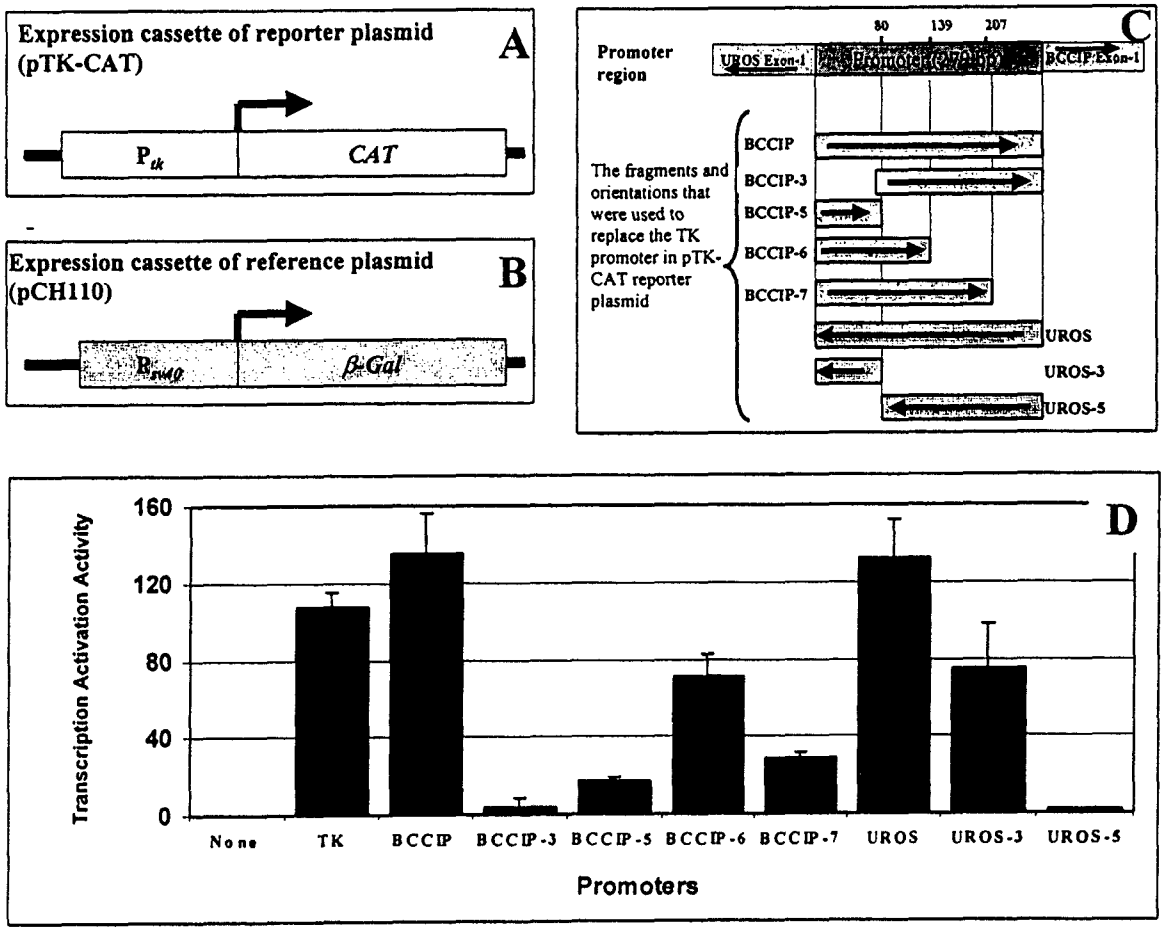

Meng, et al. Figure 4.

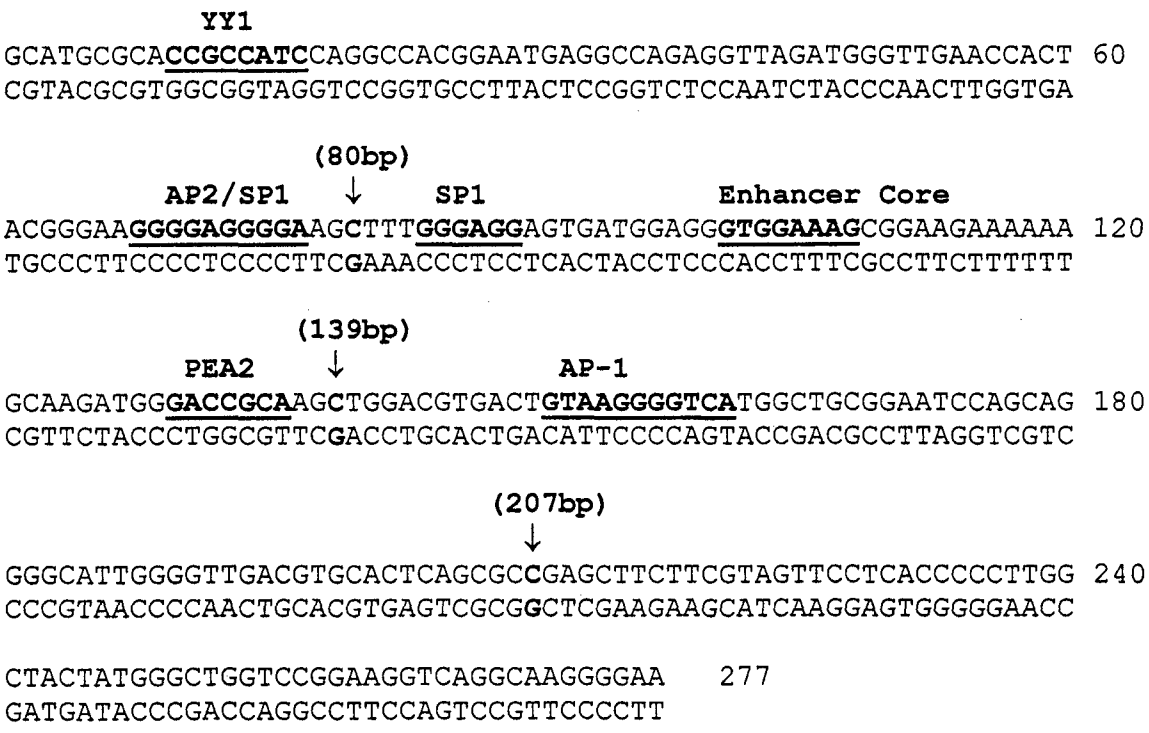

Meng, et al. Figure 5.

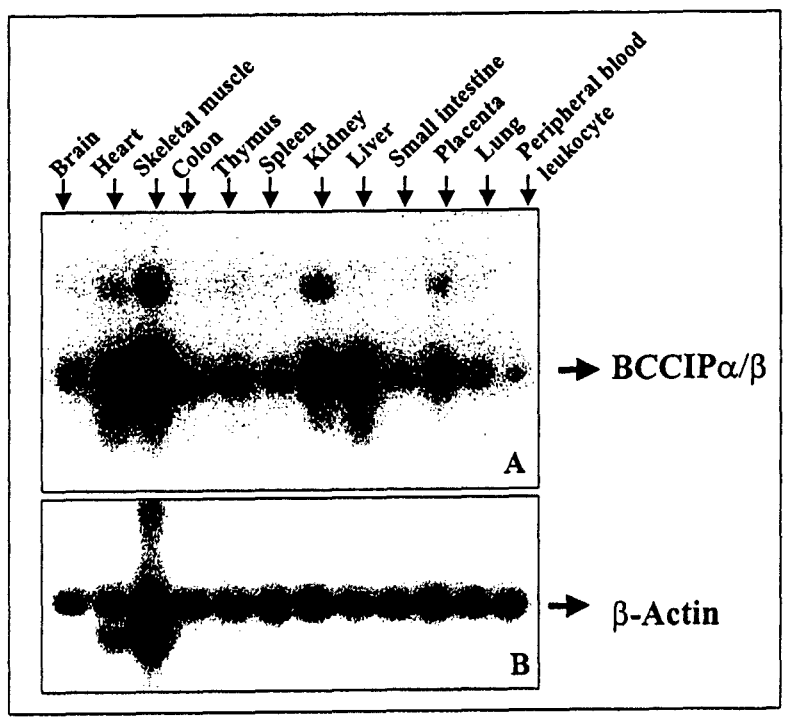

Meng, et al. Figure 6.

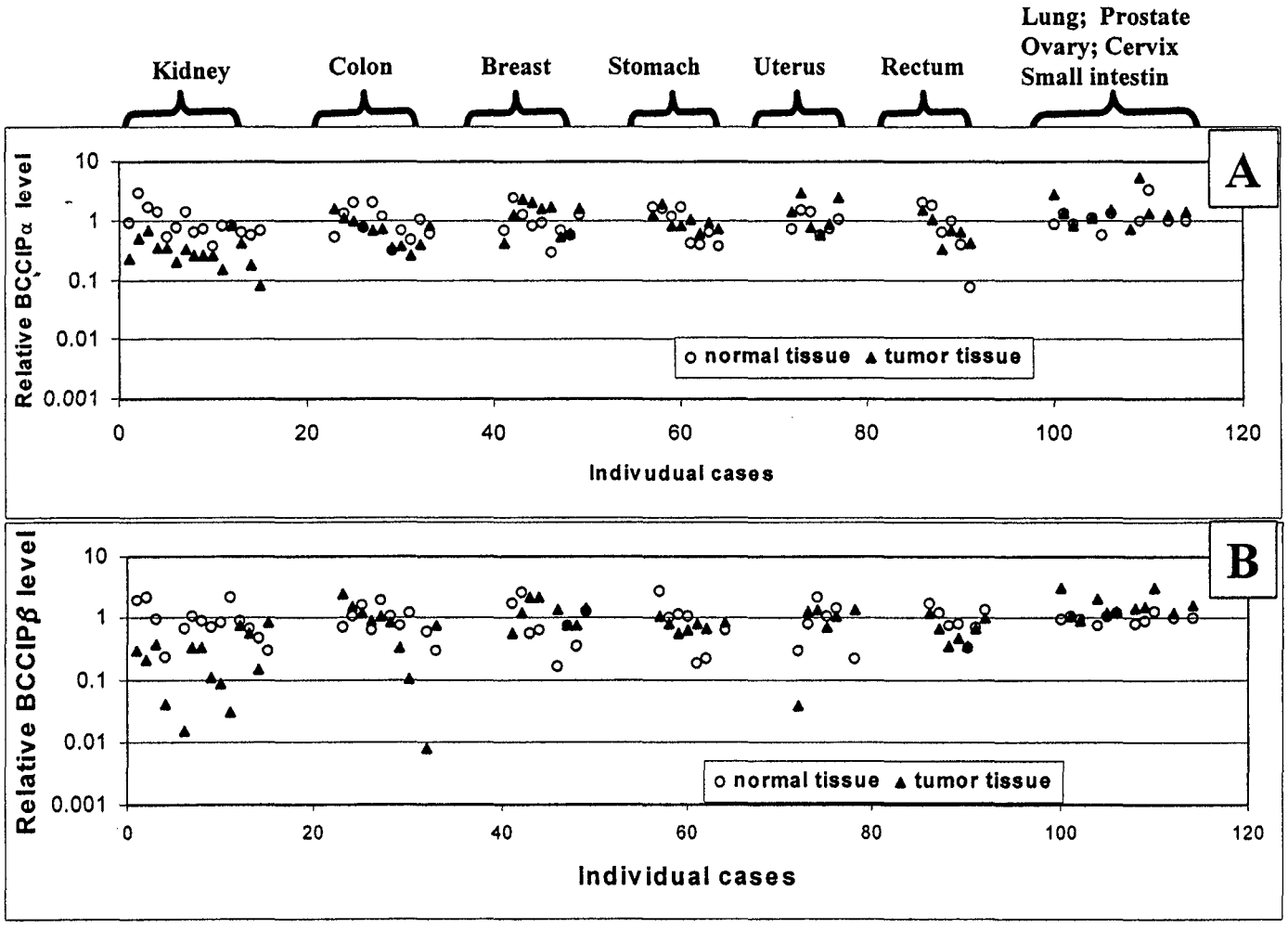

Meng, et al. Figure 7.

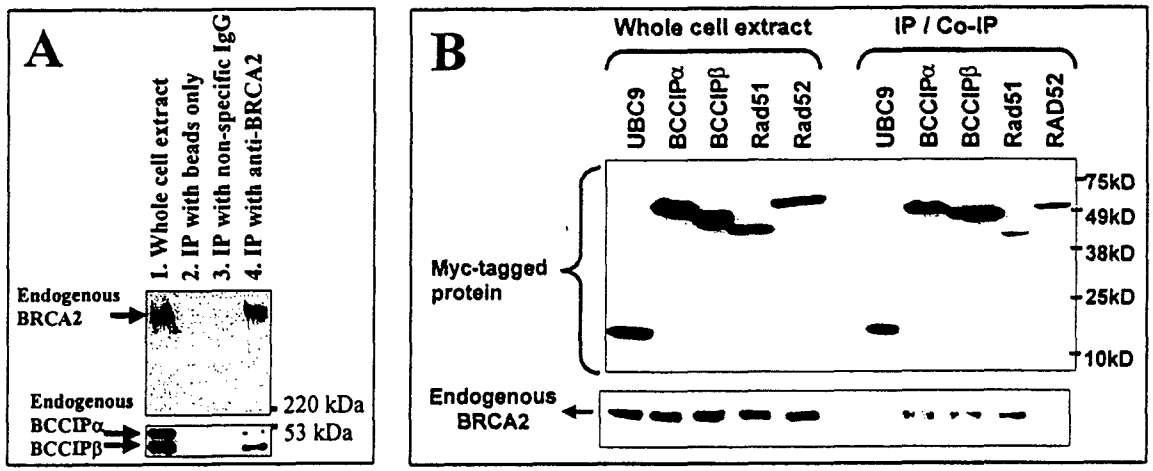

Meng et al. Figure 8.

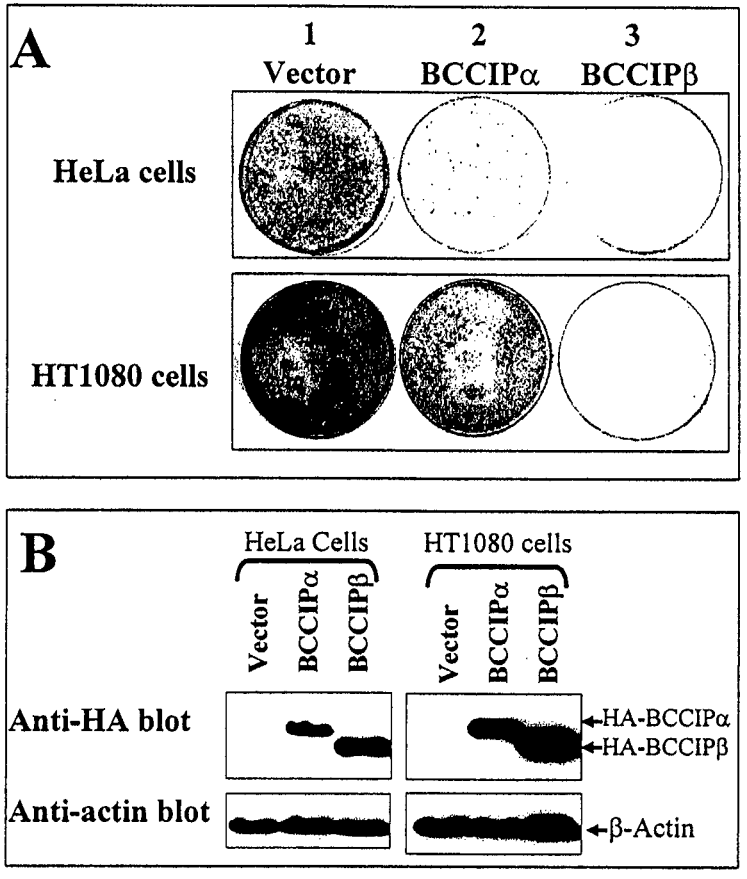

Meng et al. Figure 9.

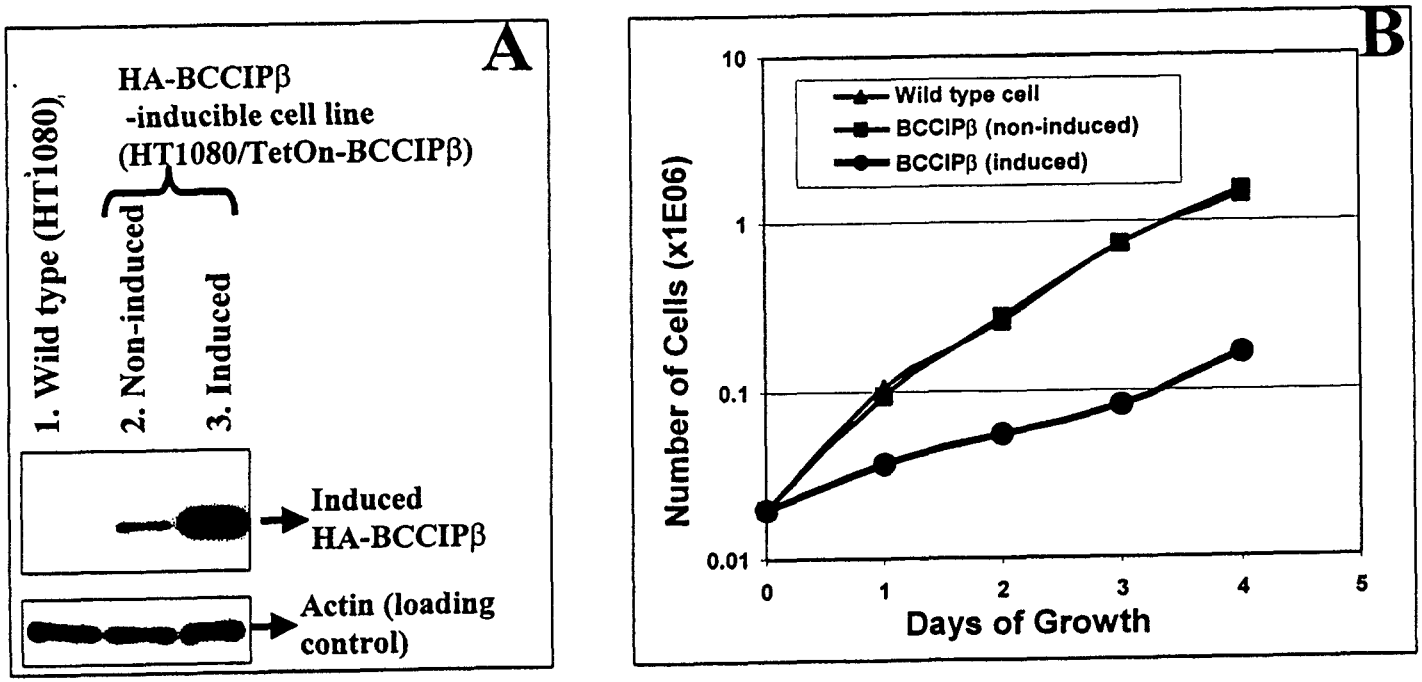

Meng et al. Figure 10.

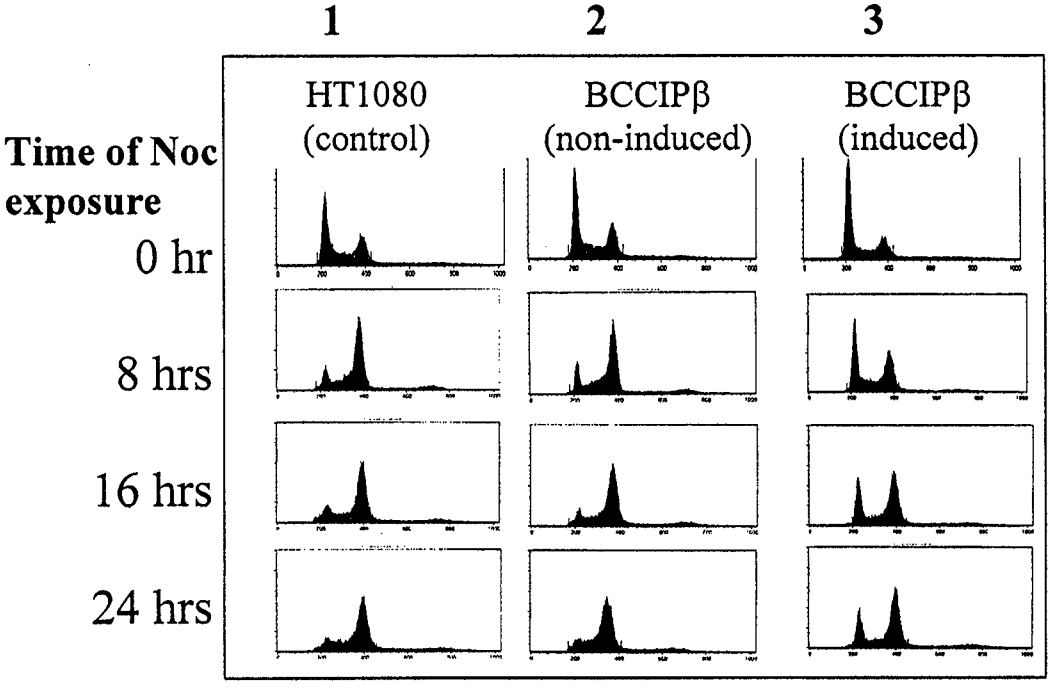

DEPARTMENT OF THE ARMY
US ARMY MEDICAL RESEARCH AND MATERIEL COMMAND
504 SCOTT STREET
FORT DETRICK, MD 21702-5012

REPLY TO
ATTENTION OF

MCMR-RMI-S (70-1y) 15 May 03

MEMORANDUM FOR Administrator, Defense Technical Information Center (DTIC-OCA), 8725 John J. Kingman Road, Fort Belvoir, VA 22060-6218

SUBJECT: Request Change in Distribution Statement

1. The U.S. Army Medical Research and Materiel Command has reexamined the need for the limitation assigned to technical reports written for this Command. Request the limited distribution statement for the enclosed accession numbers be changed to "Approved for public release; distribution unlimited." These reports should be released to the National Technical Information Service.

2. Point of contact for this request is Ms. Kristin Morrow at DSN 343-7327 or by e-mail at Kristin.Morrow@det.amedd.army.mil.

FOR THE COMMANDER:

Encl

PHYLIS M. RINEHART
Deputy Chief of Staff for
Information Management

ADB266022
ADB260153
ADB272842
ADB283918
ADB282576
ADB282300
ADB285053
ADB262444
ADB282296
ADB258969
ADB269117
ADB283887
ADB263560
ADB262487
ADB277417
ADB285857
ADB270847
ADB283780
ADB262079
ADB279651
ADB253401
ADB264625
ADB279639
ADB263763
ADB283958
ADB262379
ADB283894
ADB283063
ADB261795
ADB263454
ADB281633
ADB283877
ADB284034
ADB283924
ADB284320
ADB284135
ADB259954
ADB258194
ADB266157
ADB279641
ADB244802
ADB257340
ADB244688
ADB283789
ADB258856
ADB270749
ADB258933
ADB265793
ADB281613
ADB284934
ADB263442
ADB284977
ADB263437
ADB265310
ADB281573
ADB250216
ADB258699
ADB274387
ADB285530